Discussion

New ring culture method supports stable LR identity in cultured presomite rabbit embryos

In the first part of this study, a new culture technique, the so-called ring culture, was developed in which a medium-filled plastic ring is placed upon the extraembryonic tissue of the explanted embryo (Fig. 2). In contrast to the semi-dry standard culture method, this setting corresponds more to the *in vivo* conditions of 7.5 to 8.0 day old gastrulating/neurulating rabbit embryos in the uterus. Here, embryos lie ectoderm down on the uterus mucosa exposing their ventral surface to the fluid-filled space of the bulging implantation site. During these stages of development the ventral surface of the embryo exposed to the uterine fluid not only consists of endoderm but also of the developing axial mesoderm emerging from under its initial endodermal cover. As axial mesoderm comprises the posterior notochord (PNC), a structure considered being the laterality coordinator, the correct development of which is crucial for the stable culturing of presomite embryos (discussed below; Blum et al., 2007; Blum et al., under review). These improved settings of the ring culture, however, facilitated normal development of LR asymmetry in most cases as revealed by left-sided expression of marker genes from stage 5 onwards (Fig. 3, 4). These findings add yet another point to the growing list of advantages of the rabbit as a mammalian model organism. Besides the relatively large size of gastrulating/neurulating embryos, the development via the archetypical flat blastodisc and the only superficial implantation into the uterus mucosa, the option to stably culture presomite embryos also opens further experimental possibilities. Mouse embryos for example are difficult to culture *in vitro* and sometimes develop disturbed laterality when cultured from presomite stages onwards (Tsang et al., 1999). As cilia-driven leftward flow is already

established during early somite stages and the Nodal signalling cascade is active from the 3 somite stage onwards, the time window for experimental manipulation is very narrow. Culturing from presomite stages onwards therefore expands this time window considerably. The procedure to first culture, then record cilia-driven fluid flow and evaluate gene expression afterwards is also complicated in mouse embryos. The cup-shaped egg cylinder is not as easy accessible and does often not remain intact after filming. To further expand experimental options it might be useful to try to adapt techniques like sono- or electroporation to whole rabbit embryos to combine genetic manipulation with the existing improved culture method.

Cilia-driven leftward flow is disturbed in standard-cultured presomite embryos

The new ring culture described in this study represents an improved version of the semi-dry standard culture system (Fig. 2). Embryos cultured with the standard culture method mostly show altered LR marker gene expression after culture when explanted before the 2 somite stage. Subsequent analysis presented here could show that this was due to impaired development of the posterior notochord (PNC; Fig. 5). The PNC represents the caudal widening of the posterior notochordal plate of the rabbit blastodisc, homologous to the distal indentation of the mouse egg cylinder commonly referred to as “node” (Blum et al., 2007). In other vertebrate species equivalent structures have been identified as well: the gastrocoel roof plate in amphibians (GRP; Essner et al., 2002; Shook et al., 2004; Blum et al., 2006; Blum et al., under review) and Kupffer’s vesicle (KV) in teleost fish embryos (Essner et al., 2002; Essner et al., 2005; Kramer-Zucker et al., 2005; Okada et al., 2005; Hirokawa et al., 2006). This evolutionary conserved entity is characterised by the framing paranotochordal expression domain of *Nodal*, its epithelial organisation and the possession of motile monocilia. Laterality is conveyed from the PNC by the establishment of a laminar leftward fluid flow produced by conically rotationg monocilia. The PNC is regarded as a laterality coordinator (Blum et al., under review)

and its cellular morphology is critically related to the emergence of leftward flow and subsequent setup of LR marker gene expression.

A prerequisite for the creation of a leftward flow by cilia rotating conicallly is the localisation of the individual cilium to the posterior pole of each cell (Cartwright et al., 2004). In the rabbit, mouse and *Xenopus* it was shown that cilia are first positioned medially on the cell surface and only become progressively localised to the posterior margin of the cells concomitant with development of the PNC/GRP and the evolution of a laminar flow (Okada et al., 2005; Feistel and Blum, 2006; Schweickert et al., 2007). Due to the medial position and shortness of cilia in rabbit presomite stages a flow is never achieved in these stages (A. Rietema, personal communication; Feistel and Blum, 2006). First fluid movements manifest with the beginning of somitogenesis as local vortices and a slow, turbulent flow can be observed at the 1-2 somite stage. A laminar fluid flow then forms during the 2-3 somite stage concomitant with progressive lengthening and polarisation of cilia (supl. Fig 1; A. Rietema, personal communication; Feistel and Blum, 2006). The successive polarisation of PNC cilia most probably only starts when notochordal cells emerge from under the endoderm.
SEM analysis of embryos taken into culture at presomite stages and cultured with the standard method presented here demonstrated that PNC development was impaired in these embryos (Fig. 5). Instead of 74% of cilia in the wild type and 68% in the ring-cultured embryo only 40% of cilia in the standard-cultured embryo were localised to the posterior of cells. Additionally, the number of cells bearing no cilium was increased in these embryos. This might indicate that standard-cultured presomite embryos mostly do not establish a mature notochord and PNC although the embryo develops relatively normal to somite stages. Caused by the lack and mis-localisation of cilia in standard-cultured embryos, cilia-driven leftward flow across the PNC was disturbed (Fig. 6). Instead of showing direction toward the left side standard-cultured embryos either showed no flow or it pointed toward the posterior of the embryo (Fig. 5). In cases where almost no flow could be recorded the notochord had not surfaced properly from its initial endoderm/hypoblast cover, whereas flow, showing direction toward the posterior might be due to the mis-localisation of PNC cilia. Although the

flow of these embryos displayed some direction toward the posterior the calculated value for directionality or quality of particle movement (rho) always was very low. Rho can assume the value 1 if all particle trails analyzed represent exactly straight lines aiming in the same direction and 0 if trails show completely random direction. This value was calculated for the particle trails of each film by the program coded by Thomas Weber in statistical-R (described in the *Methods* section). The particle trails analyzed in films of standard-cultured embryos never reached a rho value of 0.4 whereas the flow of wild type embryos covered a range of 0.51 to 0.69. In ring-cultured embryos however, an even wider range of rho values was detected reaching from 0.35 to 0.75. As two of the three embryos with a rho value of below 0.4 displayed altered marker gene expression a rho of 0.4 seems to represent a threshold for the correct bias of laterality (Supplementary Fig. 1). Therefore, with a rho value above 0.4 the flow should be robust enough to ensure left-sided marker gene expression presuming that it shows direction toward the left side and, most importantly, no downstream event is perturbed. Flow with rho values between 0.3 and 0.4 instead seems not to be sufficient for left-sided marker gene expression. Hence, expression is randomised in these embryos.
Defective leftward flow due to mis-localised cilia has also been shown for *Inv* mutant mice (Okada et al., 1999; Okada et al., 2005). In these mice nearly 20% of cilia are tilted anteriorwards resulting in a slow and turbulent flow. Although more variable, the phenotype of standard-cultured rabbit embryos seems to be more severe yielding, if at all, flow that points toward the posterior whereas in *Inv*$^{-/-}$ embryos still direction toward the left side is achieved. Also the resulting LR defects are quite distinct as *Inv* mutants display completely inversed laterality whereas standard-cultured presomite rabbit embryos mostly show bilateral expression of marker genes. Nevertheless, the rho value of the flow observed in *Inv* mutants should be considerably lower than in wild type littermates as well.

The correct arrangement of cilia on the cell surface is therefore critical for the setup of flow and molecular laterality. Such coordinated polarisation of cilia within the plane of an epithelium can be achieved by the planar cell polarity pathway (PCP). In the

neural plate and inner ear, for example, components of the noncanonical Wnt/PCP pathway control planar polarity (Ybot-Gonzalez et al., 2007a; Simons and Mlodzik, 2008). Recent work in *Xenopus* has also shown that PCP-effector genes are linked to ciliogenesis (Park et al., 2006; Park et al., 2008) and that Inv might function as a switch between canonical and noncanonical Wnt signalling (Simons et al., 2005). However, mouse mutants of core PCP components do not show obvious LR defects (Lee and Anderson, 2008). Although it could be possible that this has escaped notice so far or otherwise might be due to the high redundancy between PCP components that would require the generation of double or triple knockouts. Still, it might be informative to examine the localisation of PCP components in the rabbit notochord, especially of standard-cultured presomite embryos.

In vivo, the 7.5-8.0 day old gastrulating/neurulating rabbit embryo is fixed at the margin of its uterus implantation site. Thereby the extraembryonic tissue provides a certain amount of tension to the developing embryo. This tension is lost in the setup of the standard culture whereas in ring-cultured embryos tension is provided by the ring as it is placed around the embryo onto its extraembryonic tissue. The amount of tension applied to the embryo has been described to be crucial to the development of chick embryos in culture as well (Chapman et al., 2001). It is therefore tempting to speculate that the right amount of tension is needed to support appropriate maturation of the notochord and PNC.
The artificially applied tension to the embryo might also explain the reoccurring of altered laterality in embryos taken into culture at the 1 and 2 somite stage in contrast to the completely stable stage 6 (Fig. 4). At the 1 and 2 somite stage cilia-driven leftward flow has already started or is fully developed respectively. Any falsely applied tension might therefore perturb the flow, which then could not be corrected in time.

The most peculiar finding of the present study was that cilia grew longer in ring-cultured embryos (Fig. 5). Measurements of cilia length in scanning electron micrographs (SEM) as well as in pictures of immunohistochemistry (IHC) against

acetylated tubulin showed that cilia of untreated ring-cultured embryos were about 1µm longer than in corresponding stages of wild type or standard-cultured embryos. Generally, the high standard deviation of these measurements is presumably not corresponding entirely to the *in vivo* conditions because in two-dimensional depictions the depth cannot be included in the measurement. Despite this slight inaccuracy of the measurement, the average length of cilia in ring-cultured embryos still was considerably higher than in wild type or standard-cultured embryos. One possible explanation might lie in the viscosity of the medium. The uterine fluid surrounding the embryo *in vivo* has a slightly higher viscosity than the culture medium used for *in vitro* culture. Therefore, cilia length *in vivo* might be controlled by a feedback mechanism regulated by the friction the growing cilium encounters during movement through the slightly viscous fluid (Mitchell et al., 2007). A setting in which the medium displays a lower viscosity would then impair this feedback mechanism and lead to excessive growth of cilia. As Rfx3 is a transcription factor controlling ciliogenesis (Bonnafe et al., 2004) its expression might be up-regulated in ring-cultured rabbit embryos compared to corresponding wild type stages. Another experiment to test this hypothesis would be to measure cilia in embryos cultured in the presence of methylcellulose, which renders the medium highly viscous.
That cilia in standard-cultured embryos did not show the same increase in length might be due to the comparatively small amount of medium above the embryo's ventral side during the course of culture in the standard culture setting.

Cilia-driven leftward flow is required for the establishment of laterality in rabbit embryos

That cilia-driven leftward flow per se is also required for the establishment of laterality in rabbit embryos could be shown by blocking it with methylcellulose-containing medium (Fig. 7). The added methylcellulose renders the culture medium far more viscous, thus preventing the formation of a laminar flow. This led to disturbed marker gene expression in a very high percentage of treated embryos. Mainly, expression of *Nodal* or *Pitx2* was bilateral or completely absent whereas expression exclusively on

the left or right side was encountered only rarely. Mice and zebrafish embryos deficient of Lrd (left-right dynein), which is indispensable for cilia motility, harbour immotile cilia at their PNC/KV and thus are not able to produce a leftward fluid flow. In these embryos the absence of leftward flow leads to randomised marker gene expression (Supp et al., 1997; Essner et al., 2005). In *Xenopus* however, blocking of cilia-driven flow by injection of methylcellulose resulted mostly in lack of marker gene expression (Schweickert et al., 2007). This might be explained by the force used for the injection, leaving no room for the diffusion of potential laterality determinants, whereas in rabbit, although the culture medium is removed before the addition of methylcellulose surely a thin film of medium still remains underneath the methylcellulose. This also might be owed to the different topology of the rabbit PNC, being convex with lateral furrows while the *Xenopus* GRP is relatively flat. In summary, the comparison of “no-flow situations” between rabbit, mouse, zebrafish and *Xenopus* indicate that different experimental designs might lead to different outcomes. Nevertheless in all cases the correct establishment of leftward flow is crucial for the development of laterality.

In rabbit methylcellulose treatment did not yield laterality defects in embryos treated from the 3 somite stage onwards (data not shown). This is also consistent with findings in zebrafish and *Xenopus*. The ablation of KV had no effect on heart situs and marker gene expression from the 10 somite stage onwards and the injection of methylcellulose became ineffective at stage 19/20, respectively (Essner et al., 2005; Schweickert et al., 2007). In all three species this represents the time point at which the Nodal signalling cascade with its strong positive feedback loop is already initiated (Rebagliati et al., 1998; Fischer et al., 2002; Ohi and Wright, 2006).

Different effects of unilateral Sonic hedgehog (Shh) gain-of-function in chick and rabbit

Examining Shh signalling in the rabbit embryo was of interest for two reasons: First, it was published that Shh could be transported toward the left side via cilia-driven leftward flow in the mouse (discussed below; Tanaka et al., 2005) and second, it was shown in a groundbreaking paper by Levin et al. (1995) that Shh-expressing cells ectopically placed on the right side of Hensen's node of stage 4 chick embryos induce *Nodal* expression on the right side. One aim of this work therefore was to test whether ectopic placement of Shh could influence laterality in rabbit embryos. The rabbit serves as a good model here since it is comparable to both chick as well as human development as it develops via a flat blastodisc. Surprisingly, right-sided induction of marker gene expression upon implantation of Shh protein-loaded beads was only observed in rabbit embryos explanted at the 2 somite stage (Fig. 12). In order to rule out the possibility that the observed differences were due to the experimental design (implantation of Shh-expressing cells vs. protein-loaded bead) the experiment was repeated with chick embryos and Shh protein-loaded beads. With the same protein and concentration a strong induction of *Nodal* expression was detected when beads were implanted on the right side of Hensen's node at stage 4 chick embryos (Fig. 13). Furthermore, it could be shown for the first time that this inductive effect persists until up to the 1-2 somite stage and that it applies for *Pitx2* as well (not shown). This clearly indicated that the experimental design was not responsible for the different outcome of the two experiments.

The difference between Shh signalling in rabbit and chick thus seems to be the integration of cilia-driven fluid flow. Cilia-driven flow has not been described in chick embryos up to now. The absence of flow in chick embryos might be explained by their lack of superficial mesoderm (Shook et al., 2004). The notochord of chick embryos develops as a rod-like structure, always being covered by endoderm (i.e. not superficial), whereas in rabbit embryos the notochordal plate surfaces from under its initial endodermal cover (Feistel and Blum, 2006; Blum et al., 2007). Therefore, a

superficial epithelially organised, cilia-bearing notochord free of endoderm is not formed in chick embryos (Männer, 2001). Surprisingly, this is also the case in pig embryos (Feistel, 2006). The apparent lack of superficial mesoderm of course does not rule out the possibility that a specialised structure exists elsewhere, but as in all other species examined to date the structure producing the flow is framed by the paranotochordal domain of *Nodal* (Blum et al., 2007), this seems unlikely. Instead, Hensen's node of chick and also pig embryos becomes morphologically asymmetric during late stage 4 when the primitive streak has reached its full length (Cooke, 1995; Feistel, 2006). The molecular mechanisms of the morphogenetic process responsible for node asymmetry have not been elucidated up to now. However, this morphological asymmetry precedes the asymmetric expression of *Shh* and other genes within Hensen's node (Dathe et al., 2002). The left-sided expression of *Shh* in turn leads to the induction of the paranotochordal domain of *Nodal* expression exclusively on the left side and subsequently to the initiation of Nodal in the left lateral plate (Levin et al., 1995). The molecular asymmetries present at the midline thus are sufficient to reliably induce the Nodal signalling cascade and the cilia-driven flow-module can be omitted. In agreement with this notion, all model organisms displaying a bilateral paranotochordal *Nodal* domain (mouse, rabbit, *Xenopus*, zebrafish and medaka) feature superficial mesoderm and cilia-driven fluid flow framed by *Nodal* expression (Nonaka et al., 1998; Fischer et al., 2002, Okada et al., 2005; Schweickert et al., 2007; Essner et al., 2005; Long et al., 2003). The loss of cilia-driven flow in chick and pig might represent a secondary event once Hensen's node became asymmetric during the course of chick and pig evolution.
The inductive relationship between Shh and Nodal therefore seems to be more direct in chick than in rabbit embryos, where Shh signalling works in conjunction with cilia-driven flow.

One possible downstream event of asymmetrically distributed Shh could be the side-specific down-regulation of *Coco*, a member of the Cerberus/Dan-family of secreted TGFβ-antagonists. In *Xenopus*, *Coco* has been described to be essential specifically on the right side of the embryo, assigning a repressive function on the Nodal

signalling cascade to *Coco* (Vonica and Brivanlou, 2007). It is co-expressed in the paranotochordal domain of *Nodal* and only very recently it could be shown that this domain becomes asymmetric concomitant with leftward flow (Eberhardt, 2008). Interestingly, stronger expression on the right side could be observed in a significantly smaller proportion of embryos if flow was blocked by injection of methylcellulose or cilia were rendered immotile by injection of *lrd*-antisense-morpholino (Eberhardt, 2008). These data therefore strongly suggest that *Coco* is down-regulated on the left side concomitant with the flow or rather by a signalling molecule like Shh transported by the flow. *Coco* orthologues have already been described in mouse (*Cerl-2*; Marques et al., 2004) and zebrafish (*Charon*; Hashimoto et al., 2004) to be expressed in the paranotochordal domain and to have a repressive function on Nodal signalling as well. It is therefore tempting to speculate that a rabbit orthologue exists, too. If this is the case the aforementioned hypothesis could be tested in rabbit embryos first by verifying if the expression pattern becomes asymmetric concomitant with leftward flow, i.e. in the 2-3 somite stage. Secondly, embryos could be cultured in the presence of methylcellulose to analyse if the bias of the expression is causally dependant on flow. Finally, using Shh-loaded beads implanted onto the right side of the PNC, it could be tested if *Coco* expression is influenced by Shh signalling.

The 2 somite stage in rabbit is important

Earlier work in rabbit showed that the 2 somite stage is especially important with respect to the establishment of the LR axis (Feistel and Blum, 2008). The 2 somite stage is so decisive because it is the stage in which laminar leftward fluid flow is first established which, in turn, is needed to attenuate gap-junctional communication unilaterally in order to allow for release of FGF8-mediated repression and therefore initiation of Nodal signalling. In the mouse it has been shown that membranous vesicles called Nodal vesicular parcels (NVPs) released by PNC cells are transported toward the left side by the flow (Tanaka et al., 2005). These NVPs are released upon

an FGF signal, contain Shh and retinoic acid (RA) and are supposed to be fragmented at the left side of the PNC to trigger an increase in Ca^{2+} levels. Presuming that NVPs exist in rabbit as well, this process might provide an explanation for ectopic *Nodal* induction by Shh only in the 2 somite stage. Because only at the 2 somite stage the fluid flow becomes robust and laminar enough to transport NVPs to the left side, thereby defining the time window of their potential effect. Likewise ectopically placed Shh protein would only be effective at the 2 somite stage in conjunction with the flow.

In the mouse, membrane-sheathed NVPs are described to have a diameter of 0.3-5µm and are easily recognisable in scanning EM pictures because of their high abundance (Tanaka et al., 2005). In rabbit however, SEM pictures of the PNC do not show such vesicular structures in the same amount and size (Fig. 5A; Feistel and Blum, 2006). Still, smaller particles in a much lower abundance do appear on the PNC and it would be pivotal to characterise these in greater detail. For example, this could be done by immunogold labelling of Shh protein recognised by the specific anti-Shh antibody 5E1 and subsequent analysis by transmission electron microscopy (TEM) as done in the study published by Tanaka and colleagues (2005). This would reveal if Shh is associated with membranous particles on the PNC in the rabbit as well. As vesicular particles are also seen in *Xenopus* (Schweickert et al., 2007), it would be informative to examine if Shh is linked to these, too.

One unsettled issue with the NVP model clearly is the as yet missing of an obvious asymmetric readout of Shh signalling, which should be present if Shh is transported toward the left side via the flow. As the expression of the Hh-receptor *Patched* (*Ptc*) is up-regulated in response to signalling its expression level is widely used as a readout for Shh signalling. In chick embryos, as a consequence of the asymmetric expression of *Shh,* an asymmetric *Ptc* expression can be detected (Pagán-Westphal and Tabin, 1998). In contrast, no asymmetries in *Ptc* expression have been reported in mouse (Zhang et al., 2001) or in rabbit (Fischer, 2002; Fig. 14). But maybe existing asymmetries could be detected in these species on protein level with a specific antibody against Ptc.

The involvement of cilia in Hh signalling

Besides the Shh-loaded NVPs transported by cilia-driven flow, it has been shown that cilia themselves are involved in Shh signalling in the mouse (Huangfu and Anderson, 2006). This became evident by the puzzling notion that mutations in genes of the intraflagellar transport (IFT) machinery as well as other ciliary motor proteins cause phenotypes like limb patterning defects or loss of ventral cell types in the neural tube, suggestive of defective Hh signalling (Huangfu et al., 2003; Huangfu and Anderson, 2005; Liu et al., 2005; Houde et al., 2006). Subsequently, it could be shown that Smo localises to cilia upon a Shh signal (Corbit et al., 2005) and that several other components of Hh signalling like the Gli transcription factors, Ptc and Sufu also localise to cilia (Haycraft et al., 2005; Rohatgi et al., 2007). Interestingly, it could recently be shown that these components of the Hh signalling machinery can also be detected on primary cilia on undifferentiated human embryonic stem cells (Kiprilov et al., 2008). As Shh seems to be transported in NVPs via cilia-driven flow it might therefore make sense that Hh signalling components become enriched on cilia. It would thus be very interesting to know if those components localise to cilia in rabbit embryos as well. This could be done by the use of specific antibodies against these proteins in whole mount immunohistochemistry. Chick embryos might not possess cilia-driven leftward flow but, of course, are not devoid of cilia (Männer, 2001). It would thus be very interesting as well to examine if Hh signalling components are coupled to cilia in chick embryos.

Inhibition of Shh signalling leads to loss of midline barrier

The inhibition of Shh signalling by incubation with cyclopamine caused bilateral expression of LR marker genes in rabbit embryos (Fig. 15). As Shh plays an inductive role in rabbit as well, this was an unexpected finding at first glance. Cyclopamine, a teratogenic plant alkaloid, was shown to bind directly to Smoothened (Smo), the major Hh signal transducer (Chen et al., 2002) and mice deficient for

Smoothened, which represents a complete loss of Hh signalling, show no marker gene expression in the lateral plate (Zhang et al., 2001). But as the cyclopamine treatment of rabbit embryos in culture did not yield a complete abolishment of Shh signalling, revealed by the residual expression of its target gene *Patched* (*Ptc*; Fig. 14), the results seem more comparable to *Shh* mutant mice. The phenotype of those mice is less severe than that of $Smo^{-/-}$ mice and they display bilateral expression of LR marker genes (Tsukui et al., 1999). The differing phenotype is due to the redundant function of *Indian hedgehog* (*Ihh*), which is co-expressed in the node and PNC and is still active in *Shh* mutants. This was confirmed by the similar phenotypes of *Shh*/*Ihh* compound mutants and *Smo* knockout mice (Zhang et al., 2001). As *Ihh* is expressed in the node and PNC of rabbit embryos as well (Fig. 8) the combined residual signalling activity of Shh and Ihh seems to be responsible for the observed phenotype of cyclopamine-treated embryos.
Subsequent analysis of this phenotype could also show that the bilateral expression of marker genes was due to a loss of *Lefty* expressing floor plate cells (Fig. 16). In the mouse it has been described that the loss of the Nodal feedback inhibitor *Lefty1*, normally expressed in the left side of the floor plate, leads to bilateral expression of *Nodal*. Hence, it was concluded that *Lefty1* most probably exerts a midline barrier function preventing the spreading of signals from the left side toward the right side (Meno et al., 1998, Yamamoto et al., 2003). Additionally, it could be shown that Shh signals from the notochord are required for the induction of the floor plate (Roelink et al., 1994) and that consequently, Shh mutant mice are not able to specify a floor plate, which leads to a secondary loss of restrictive *Lefty* expression (Chiang et al., 1996; Tsukui et al., 1999; Meyers and Martin, 1999). Thus, the loss of floor plate cells and Lefty expression in cyclopamine treated rabbit embryos completely resembles the loss of Shh in the mouse.

In *Smo* knockout mice it was shown that Hh signalling regulates the paranotochordal expression of the TGFβ growth factor Gdf1 (Zhang et al., 2001). In the absence of Hh signalling in $Smo^{-/-}$ mice the paranotochordal domain of Gdf1 is down-regulated compared to wild type littermates. In rabbit embryos this particular expression

domain could not be detected by whole mount *in situ* hybridisation (Fig. 11). This was surprising because all other genes associated with Hh signalling analyzed in rabbit embryos in this study resembled relatively closely the described expression patterns in mouse (*Ihh*, *Smo*, *Hip*; Figs. 8-10). But as the authors of the mouse studies used a probe consisting of the complete coding sequence of the mouse *Gdf1* gene (Rankin et al., 2000; Zhang et al., 2001), the 660bp fragment used in the present work might not be able to visualise the paranotochordal expression domain of *Gdf1* in the rabbit. Therefore, it should be attempted to clone the complete coding sequence in rabbit as well as this might allow for better visualisation of the *Gdf1* expression pattern.

Dual function of FGF8 signalling in the rabbit

In the present work it was shown that in early stages FGF8 signalling is required to render the lateral plate competent for the Nodal signalling cascade. Another important result was that FGF8 signalling is not involved in ciliogenesis or the set-up of cilia-driven leftward flow in rabbit embryos. Finally, it was shown that FGF8 is epistatic to leftward flow and is involved in the transfer of LR cues during the 2 somite stage.

FGF8 signalling renders the lateral plate competent for Nodal signalling

Systemic inhibition of FGF8 signalling by incubation with SU5402 led to a loss of asymmetric marker gene expression in embryos explanted prior to the 2 somite stage (Fig. 17). SU5402 is a compound disrupting FGF8 signalling by specifically interfering with the catalytic centre of the FGF receptor 1 (FGFR1; Mohammadi et al., 1997). That FGFR1 is the major transducer of FGF8 signalling among the four existing FGF receptors was inferred from the phenotypic resemblance of FGF8 and FGFR1

mutants in mouse, zebrafish and medaka and SU5402 has since been widely used as a specific inhibitor of FGF8 signalling (Yamaguchi et al., 1994; Sun et al., 1999; Yokoi et al., 2006).

The lack of marker gene expression in SU5402-treated embryos was a surprising finding because it has been shown in previous studies that a SU5402-loaded bead implanted on the right side of the PNC could induce ectopic marker gene expression (Fischer et al., 2002; Feistel and Blum, 2008). Therefore, the expected outcome of systemic inhibition of FGF8 signalling was rather bilateral expression than loss. One possible explanation for this could be a dual, temporally separated function of FGF8 signalling. The implantation of an SU5402-loaded bead only induced ectopic expression in the 1-2 somite stage (Fischer et al., 2002), whereas the systemic incubation led to loss of marker gene expression only prior to the 2 somite stage (Fig. 17). During the 2 somite stage systemic SU5402 treatment caused bilateral expression as well and loss of expression was never observed. This might indicate that during the 2 somite stage systemic inhibition mimics the effect of right-sided bead implantation but another function of FGF8 signalling is compromised by earlier inhibition leading to a loss of asymmetric expression. The competence to express the Nodal signalling cascade in the lateral plate is thought to be mediated by the paranotochordal domain of *Nodal* (Brennan et al., 2002; Saijoh et al., 2003). Interestingly, in *Xenopus* embryos systemic inhibition of FGF8 signalling by SU5402 caused loss of marker gene expression as well (Schneider, 2008). Subsequent analysis showed that the paranotochordal *Nodal* domain was missing or greatly reduced in these embryos. Moreover, in hypomorphic $FGF8^{neo/-}$ compound mouse mutants, the paranotochordal domain only appears as scattered cells and the lateral plate expression is also not initiated (Meyers and Martin, 1999). Taken together, this might indicate that FGF8 is responsible for the set-up of the paranotochordal *Nodal* domain subsequently conferring competence to the lateral plate. Interestingly, preliminary data from *Xenopus* suggest that the gain-of-function of FGF8 signalling conversely causes an up-regulation of the paranotochordal *Nodal* domain, further highlighting the implication of FGF8 signalling in the set-up of this domain (T. Beyer, personal communication).

Although the paranotochordal *Nodal* domain of SU5402-treated rabbit embryos seemed reduced in some specimens, a clear correlation compared with the DMSO-treated controls could not be established, also because this domain shows some variability after *in vitro* culture even in untreated control embryos. It might therefore be more informative to analyse expression levels by RT-PCR of isolated paranotochordal tissue. This would also eliminate possible variations caused by the *in situ* hybridisation method, as for example the length of Proteinase K treatment causes differences in signal intensity afterwards.

FGF8 signalling is not involved in ciliogenesis in the rabbit

Systemic inhibition of FGF8 signalling by SU5402-supplemented culture medium did not influence the development of the ciliated epithelium of the PNC or the dynamics of leftward flow produced by PNC cilia compared to DMSO- or untreated control embryos (Fig. 18). Additionally, the length of PNC cilia did not seem to be affected by this treatment (Fig. 18). SU5402 is a compound specifically interfering with FGF-receptor 1 signalling and thus FGF8 signalling (discussed above; Mohammadi et al., 1997).

In zebrafish it was recently suggested that incubation with SU5402 as well as injection of an antisense-morpholino against FGF-receptor 1 (FGFR1) leads to the abrogation of cilia-driven fluid flow in Kupffer's vesicle (KV; Neugebauer et al., 2008). Detailed analysis indicated that this was due to significantly shorter KV cilia. As a consequence of the loss of cilia-driven flow, the expression of the zebrafish *Nodal* homolog *Southpaw* became bilateral. It was thus concluded that FGF8 signalling regulated ciliogenesis in zebrafish. The results of the present study however, do not support a function of FGF8 in ciliogenesis in the rabbit. Although PNC cilia of different treatment groups did not show the exact same length, the parameters of the flow were not grossly altered between SU5402-incubated embryos that showed no or bilateral expression, DMSO-treated control embryos or those treated with SU5402 but exhibiting left-sided expression afterwards (Fig. 18). Most importantly, cilia of

embryos with altered marker gene expression after SU5402 treatment were not shorter than those of untreated control embryos. The observed difference in cilia length may therefore be in the normal range of ring-cultured embryos or might also be explained by the small number of embryos in which cilia were measured. To substantiate these results the experiment should be repeated to measure the length of cilia in more treated embryos.

The complete loss of *FGF8* in mouse FGF8 mutants leads to massive gastrulation defects (Sun et al., 1999). Cells of the epiblast enter the primitive streak but are not able to migrate any further causing massive bulging of the primitive streak. Consequently, almost no mesoderm is formed including axial mesodermal structures like the PNC. This severe phenotype seems to be caused by the loss of both *FGF8* and also *FGF4*, which is normally co-expressed in the primitive streak but is lost in *FGF8* mutant mice (Sun et al., 1999). Although the loss of *FGFR1* causes a less severe phenotype in mice, mesoderm differentiation is still aberrant. Axial mesodermal structures seem to form but are massively disorganised (Deng et al., 1994; Yamaguchi et al., 1994; Ciruna and Rossant, 2001) and whether cilia form on those cells is not clear. What seems to be clear instead is that signalling via FGFR1 in the mouse is responsible for the general specification of mesodermal structures and not for the more specialised process of ciliogenesis in mesodermal cells. That the phenotype of FGFR1 antisense-morpholino-injected zebrafish embryos is much less severe as the complete knockout of FGFR1 in mouse could also indicate dosage dependency. A mouse mutant in which FGF8 signalling is only partially lost is the hypomorphic $FGF8^{neo/-}$ compound mutant (Meyers and Martin, 1999). Those mutants are able to proceed relatively normal through gastrulation and form axial mesodermal structures but whether those mutants display ciliogenesis defects has not been examined as yet. Other mouse mutants that lack PNC cilia or harbour immotile/shorter ones and therefore lack leftward flow always show randomised or bilateral marker gene expression (Nonaka et al., 1998; Okada et al., 1999; Bonnafe et al., 2004). As hypomorphic FGF8 mutants instead lack asymmetric marker gene expression completely (Meyers and Martin, 1999) it might by inferred that this

phenotype is not due to abrogation of cilia-driven leftward flow because of defective ciliogenesis. Also, incubation of mouse embryos with SU5402 did not influence cilia-driven leftward flow as well (Tanaka et al., 2005). Indicating that FGF8 signalling, like in rabbit, might also not be involved in ciliogenesis in the mouse.

FGF8 signalling is epistatic to leftward flow and functions in the relay of LR cues during the 2 somite stage

The inhibition of FGF8 signalling by incubation with SU5402 suggested no causal connection between FGF8 signalling and ciliogenesis in rabbit embryos (Fig. 18; discussed above). Earlier work in rabbit has shown that FGF8 has a right-sided repressive function, which later was shown to be dependant on gap-junctional communication (GJC; Fischer et al., 2002; Feistel and Blum, 2008). From this it was concluded that FGF8 signalling plays a role in the transfer of LR cues independent of cilia-driven leftward flow (Feistel and Blum, 2008). In the present study it was tested in an epistasis experiment if FGF8 signalling was able to exert its asymmetric function in a “no-flow situation”. Therefore, embryos were cultured with an FGF8-loaded bead implanted on the left side and an SU5402-loaded bead on the right side of the PNC, covered with methylcellulose-containing medium (Fig. 19). In this setting, the FGF8 bead should block endogenous asymmetric marker gene expression, whereas the SU5402 bead should allow for ectopic right-sided expression and the methylcellulose renders the medium viscous enough to block leftward flow. Compared to embryos cultured only in the presence of methylcellulose, embryos that had received the two beads showed markedly reduced incidences of marker gene expression in the left lateral plate and an increase in expression exclusively on the right side (Fig. 19). This strongly suggested that also in a “no-flow situation” FGF8 was able to exert its repressive function and that the local inhibition of FGF8 signalling allowed for marker gene expression. These results emphasise again that FGF8 signalling is not involved in the set-up of a functional PNC and cilia-driven leftward flow in rabbit embryos. Instead these data support a model put forward in earlier work (Feistel and Blum, 2008). This model states the following: (1) from the

paranotochordal domain, a Nodal inducing signal, perhaps Nodal protein itself, spreads towards both sides, (2) FGF8 exerts repression of the Nodal signalling cascade via GJC and (3) a flow-mediated release of repression. Step (3) of course is not necessarily falsified by the above-mentioned experiment because the event terminating FGF8 signalling mediated *Nodal* repression *in vivo* could still be flow-mediated. The experiment rather showed that the signalling itself is independent of flow and that it is not affecting the set-up of flow. Including the results of the present study, the model for FGF8 signalling might be extended by the following: (1) FGF8 signalling confers competence to the lateral plate by setting up the paranotochordal expression domain of *Nodal*. (2) From this domain Nodal protein spreads towards both sides and FGF8 is needed in step (3) to repress the Nodal signalling cascade via GJC. Step (3) involves the left-sided release of repression, which might be flow-mediated, to start the Nodal signalling cascade in the left lateral plate mesoderm.

Taken together, it might be conceivable that both signalling pathways examined here, converge on the regulation of the paranotochordal domain to specify laterality, Shh by the regulation of the Nodal inhibitor *Coco* in this domain and FGF8 by the set-up of the *Nodal* domain itself.

Material and methods

Cloning of gene sequences and expression analysis

Fragments of genes of which sequence information in other species was available were cloned and analysed for their expression patterns in rabbit embryos.

RNA-Isolation from embryos

Total RNA was extracted from E12 embryos according to the Peqlab PeqGOLD TriPure^{TM} Kit. This method is based on one step-liquidphase-Separation in phenol and chloroform.

E12 embryos were dissected in PBS^{+}, immediately frozen in liquid nitrogen and stored at -80°C. For RNA-Isolation, one embryo was homogenized in 1ml of PeqGOLD TriPure^{TM} and incubated for 5 min. at RT. Afterwards 0,2ml chloroform were added and the tube was shaken vigorously for 15 sec. After another 10 min. of incubation at RT the probe was centrifuged for 5 min. at full speed to separate the homogenate into 3 phases. The aqueous phase contained the RNA, the interphase the DNA and the organic phase the proteins. For RNA-precipitation the aqueous phase was transferred into another tube and 1ml isopropanol was added. After centrifugation at full speed and 4°C the pellet was washed twice in 1ml of 75% ethanol, centrifuged briefly, dried and then resuspended in about 100µl of sterile DDW. Probes were stored at -80°C.

First strand synthesis of cDNA

cDNA was synthesized from total RNA preparations by reverse transcription using M-MLV Reverse Transcriptase. For a standard protocol, 1µg of random hexamers were added to 1µg of RNA and filled up with sterile water to a final volume of 14µl. The solution was heated to 70°C for 5 min to melt secondary structures within the template and immediate cooling on ice thereafter prevented these structures from reforming. Afterwards 5µl of 5x M-MLV Reaction Buffer, 1.25µl of 10mM dNTPs and 1µl (200 units) of M-MLV RT were added and filled up to a volume of 25µl. After an initial incubation at 10 min. at room temperature the reaction was then put to 42°C for another 50 min to complete first strand synthesis.

Polymerase chain reaction (PCR)

Oligonucleotides and PCR conditions

For the design of primers, already available sequences of interest preferably of human or mouse were run against a genomic database (NCBI Blastn) or were directly aligned to each other. Alignments derived from such searches were checked for regions of high homology and oligonucleotides of about 20-25 bases spanning regions of 500 to 1000 basepairs were designed as primers for the following PCR reactions. Usually three forward and reverse primers per gene were used to amplify products of different lengths. The primer combination giving the best PCR result was used to obtain a fragment for further amplification in bacteria.
The following primer combinations and PCR conditions were used:

Ihh

forward: for1 5’ GCC GAC CGC CTC ATG ACC CAG CGC 3’
reverse: rev1 5’ GGG GCC AGA AGG CCA ACT GAG CCA G 3’
primer concentration: 15pM/µl
annealing conditions: 68°C, 30sec; 8% DMSO

Probes against *Dhh*, *Smo*, *Hip* and *Gdf1* as well as against *Nodal*, *Pitx2* and *Lefty* were kindly provided by Dr. Anja Rietema.

Gsc (not shown):
forward: for1 5' ATG CCC GCC AGC ATG TTC AG 3'
reverse: rev2 5' CCG CGG CCG TCA GCT GTC CGA GTC C 3'
primer concentration: 15pM/µl
annealing conditions: 62°C, 30sec; 6% DMSO

Pcl2 (not shown):
forward: for4 5' CTG GAG GCA TTA AAT GAT TAC AAG 3'
reverse: rev3 5' GTT CAG TCC TAC AGT CAG GAT GC 3'
primer concentration: 20pM/µl
annealing conditions: 56°C, 30sec; 6% DMSO

Lfng (not shown):
forward: for3 5' GAG ACC TGG ATC TCG CGC CAC AAG G 3'
reverse: rev4 5' GAG CGG AAC CTG GAT GGG TC 3'
primer concentration: 15pM/µl
annealing conditions: 61°C, 30sec; 6% DMSO

Standard PCR protocol
For a 25µl PCR reaction 1µl of previously prepared cDNA was mixed with 2mM dNTPs, 1U of *Taq* DNA Polymerase, 5µl 5x Buffer, 1µl of each the forward and the reverse Primer (concentration indicated) and filled up to a volume of 25µl with sterile double distilled water (DDW). If necessary, DDW was substituted with varying amounts of DMSO (6-8%) to enhance specific hybridization of the oligonucleotides.
A standard PCR program started with (1) 1min at 95°C, followed by (2) 30sec at 95°C, (3) 30sec or 1min at the annealing temperature indicated and (4) 1min at 72°C. Steps (2) to (4) were repeated 39 times before the reaction was (5) stopped and kept

in the cycler at 8°C. Step (1) and (2) yield a denaturation of double-stranded templated DNA, step (3) allows hybridisation of the primers to the single-stranded DNA and during step (4) the *Taq*-Polymerase elongates the sequence from the primer's 3' end.
If the product was intended to be further amplified in bacteria, another 15min at 72°C were added after the 40 cycles to make use of the *Taq*-Polymerase's Terminal Transferase activity that adds an extra Deoxyadenosine onto each 3' end of the already existing double-stranded PCR product. This creates a 3' A-overhang on each side that can be utilised for ligation into a cloning vector.

Agarose gel analysis
For gel analysis of nucleic acids a standard 1% agarose gel in TAE buffer supplemented with an end concentration of 0.4µg/ml ethidium bromide solution was used. After the negatively charged nucleic acid fragments were segregated under the influence of an electrical field the gel was exposed to UV light where the fluorescence of the intercalated ethidium bromide could be visualised and documented.

Subcloning of PCR products and bacteria culture

Two different cloning systems were used to amplify PCR products: the desired sequences were either cloned into the pCRII-TOPO-vector from the TOPO TA cloning Kit and amplified in OneShot chemically competent cells (*E.coli*) or ligated into the pGEM-TEasy vector and transformed into chemically competent XL-1 blue cells (*E.coli*). Both vectors have their multiple cloning site within the coding region of β-galacosidase, so that positive clones can be selected by blue and white screening.

Ligation of PCR products into cloning vectors
The linearized pCRII vector has the enzyme topoisomerase covalently bound to 3'-T overhangs at its multiple cloning site. This enables the direct ligation of Tac-amplified PCR products with 3'-A overhangs into the vector. A cloning reaction was set up by

combining 4µl of fresh PCR product with 1µl of the provided Salt solution. To this 1µl of vector was added and the reaction was incubated for 10min at room temperature. The reaction tube was then placed on ice for the following transformation into competent bacteria.
Ligation of PCR products into the linearized pGEM-TEasy vector was facilitated by the T4 ligase. In a standard reaction, 5µl of ligation buffer, 1µl of vector and 1µl of T4 ligase were combined with 3µl of fresh PCR product. The reaction was incubated for 1h at room temperature or over night at 4°C and then transformed into bacteria.

Transformation and clonal selection
The ligated vectors were transformed into chemically competent bacteria using the heat shock method. For the TOPO TA protocol, 2µl of ligation reaction were added to just thawing competent bacteria (OneShot). This reaction was incubated for 30min on ice and then heat-shocked for 30sec at 42°C. Afterwards the reaction was again placed on ice, supplemented with 250µl of SOC medium and incubated at 37°C with shaking.
For the pGEM-TEasy transformation 5µl of ligation reaction were added to competent bacteria (XL-1 blue cells), incubated for 30min on ice and heat-shocked for 90sec at 42°C. Then, 400µl of SOC medium were added on ice and the reaction was incubated for 90min at 37°C with shaking.
After incubation at 37°C different volumes (typically 50, 100 and 150µl) of the bacteria suspension were plated on LB-agar selective plates (100µg/ml Ampicillin; 40µg/ml X-Gal for TOPO-cloning, 100µg/ml Ampicillin; 0.5mM IPTG; 40µg/ml X-Gal for pGEM-TEasy-cloning) and incubated at 37°C over night. Only white colonies, indicating the insertion of the PCR product into the multiple cloning site and hence the disruption of the β-galactosidase coding region, were selected for further amplification and analysis using the mini-prep procedure.

Preparation and handling of nucleic acids

Preparation of small amounts of plasmid DNA (mini-prep)

Plasmid DNA from *E. coli* cultures was isolated using a modified alkaline lysis protocol. All centrifugation steps were done at 4°C.

3ml of selective LB medium (100µg/ml Ampicillin) were inoculated with a single white bacteria colony of a selective plate and grown overnight at 37°C with shaking. 2ml of the culture were poured into a microcentrifuge tube and bacteria were pelleted through centrifugation at 5000rpm for 5 min. The supernatant was discarded and the pellet resuspended in 100µl of P1 buffer by heavy vortexing. Then 200µl of lysis buffer (P2) were added and the tubes were inverted several times to thoroughly mix the reagents. Alkaline lysis was allowed to proceed for 5min at RT and was then stopped by neutralising with 150µl of neutralisation buffer (P3), again inverting the tubes several times. After 20min incubation on ice, the lysate was cleared from the fluffy white precipitate containing genomic DNA, cell debris and proteins by centrifugation at full speed for 10min. 400µl of the clear supernatant were transferred to a fresh microcentrifuge tube and mixed well with 1ml of cold Ethanol to precipitate the plasmid DNA. After centrifuging for 10min at full speed the pelleted plasmid DNA was washed with 500µl of 70% Ethanol, centrifuged briefly, dried and resuspended in 50µl of sterile DDW.

Preparation of medium amounts of plasmid DNA (midi-prep)

Medium amounts of plasmid DNA were isolated following the Promega “PureYield Plasmid Midiprep System” using the vacuum method. Here, all centrifugation steps were done at RT.

100ml of selective LB medium (100µg/ml Ampicillin) were inoculated with 1ml of a positively tested bacteria culture and cultivated overnight with shaking at 37°C. Then bacteria were pelleted by centrifugation for 10min at 5000g and the supernatant was discarded. For resuspension the pellet was heavily vortexed in 3ml of Cell Resuspension Solution. Afterwards, cells were lysed by adding 3ml of Cell Lysis Solution and incubating for 3min at RT. Addition of 5ml Neutralisation Solution

stopped the lysis and after another 3min of incubation at RT the lysate was centrifuged for 10min at full speed to pellet the cell debris and protein precipitate. The clear lysate was then decanted into the Clearing Column which was fit onto the Binding Column and the Vacuum Manifold. Using the vacuum, the lysate was completely pulled through the columns and the Clearing Column was discarded. The membrane of the Binding Column to which the plasmid DNA was bound is then washed by pulling through 5ml of Endotoxin Removal Wash and 20ml of Column Wash Solution. To dry the membrane after the washing steps the vacuum was applied for another 60sec. Then, the Binding Column was removed from the Vacuum Manifold and put into a 50ml Falcon Tube. To elute the plasmid DNA 600µl of nuclease free water was added to the binding membrane and recovered by centrifugation in a swing out rotor for 5min at 1500g.

Measuring the concentration of nucleic acids

The concentration of nucleic acids in aqueous solutions was determined via spectrophotometry. The ratio of absorption (A) at the wavelengths 260nm and 280nm measured against the solvent indicated the purity of the solution (pure nucleic acid solution: 1.8 for DNA and 2.0 for RNA). The content of either DNA or RNA was inferred from the A_{260} value with 1 unit corresponding to 50µg/µl DNA and 40µg/µl RNA.

Restriction enzyme digests

To check for insertion of the correct PCR fragment after a mini-prep inserts were released from the plasmids by digestion with a restriction enzyme cutting on both sides of the multiple cloning site. EcoRI could be used for both pCRII-TOPO and pGEM-TEasy vectors. Typically 1.5µl of 10x buffer and 1µl of enzyme were added to 10µl of plasmid DNA and the mixture was filled up to a volume of 15µl with 2.5µl of sterile DDW and incubated for 2hrs at 37°C. After digestion the reaction was analysed on a 1% agarose gel.

For linearization digests usually 20µg of plasmid DNA were used in a 100µl reaction. The enzyme was concentrated according to the manufacturer's instruction and

incubated overnight at 37°C. Afterwards 1µl of the digestion was controlled against uncut plasmid DNA on a 1% agarose gel.

Sequencing and database analysis

Inserts of plasmids were sequenced at Seqlab, Göttingen. The obtained sequences were run against the NCBI database using the "blastn" algorithm. (www.ncbi.nlm.nih.gov/BLAST).

Whole mount *in situ* hybridisation

In vitro transcription of RNA probes

For *in vitro* transcription of RNA probes 0.4-1µg of linearized plasmid with the insert of interest was used as a template. Depending on the orientation of the insert 20units of either SP6 or T7 RNA polymerase were added to a mixture of template, 4µl Transcription Buffer, 0.5µl (=20units) RNasin, 2µl DTT and 2µl of digoxigenin-labelled NTPs. Sterile DDW was added to a final volume of 20µl and the mixture was incubated at 37°C for 2hrs. After transcription 115µl of cold 100% Ethanol and 3.75µl of 4M LiCl were added and the transcribed RNA was precipitated for at least 20min at -20°C. Then the tube was centrifuged at full speed and 4°C for 30min to pellet the RNA. The supernatant was discarded and the pellet was washed with 20µl of cold 70% Ethanol and centrifuged again for 5min. Afterwards the Ethanol was discarded and the pellet was allowed to dry shortly before it was resuspended in 20µl of a 1:1 mixture of sterile DDW and formamide. 1µl of the resuspended RNA probe was mixed with 8µl sterile DDW and 1µl 10x Loading Buffer and checked on a 1% agarose gel for the appropriate size and integrity of the product. The remainder of the RNA probe was stored at -80°C until further use.

In situ hybridisation

Whole mount *in situ* hybridisation was used to detect expression patterns of specific genes of interest in whole rabbit and chick embryos. Expression of newly cloned

genes was assessed in wild type embryos whereas embryos after *in vitro* culture were tested for left-right marker genes. Unless otherwise indicated, at least 3ml of buffer are used for each washing step.

Day 1: On the first day of the procedure the tissue was prepared for taking up the digoxygenin-labelled antisense RNA probe, which hybridizes to the endogenous target mRNA. Embryos were either used directly after fixation with 4% PFA (4% paraformaldehyde in PBS$^-$) or were rehydrated from storage in 100% methanol through a graded series of 75, 50 and 25% methanol in PBS$^-$w (PBS$^-$ with 0.1% Tween-20) on ice. Embryos were washed three times in PBS$^-$w for 5min and then the tissue was permeabilized for 5 to 30min with 10µg/ml proteinase K in PBS$^-$w at RT. Digestion was stopped with 2mg/ml glycine in PBS$^-$w followed by three washing steps in PBS$^-$w for 5min. The tissue was then refixed for 15min in 4% PFA supplemented with 0.2% glutaraldehyde. After washing four times in PBS$^-$w for 5min the embryos were transferred into a 1:1 mixture of hybridization solution in PBS$^-$w. After equilibration in 1ml 100% hybridization solution, a pre-hybridisation period in 900µl hybridisation solution at 65°C for 2-3 hours eliminated endogenous phosphatases. Depending on the concentration of the antisense RNA probe about 1µl was added to 100µl of hybridisation solution and the mixture was heated to 95°C for 5min to melt secondary structures. Afterwards the mixture was put on ice to prevent secondary structures from reforming and then added to the vial where the embryo was incubated with the probe at 70°C overnight.

Day 2: On the second day access antisense probe was removed in high stringency washing steps and the tissue was prepared for the incubation with the anti-digoxygenin antibody. In a first step, the hybridisation solution containing the RNA probe was replaced by 800µl of pure hybridisation solution and embryos were incubated for 5min at 70°C. In three steps 400µl of 2x SSC (pH 4.5) were added at a time and incubated for 5min at 70°C. Afterwards Embryos were washed in 2x SSC (pH7) for 30min at 70°C. The washing steps in SSC were followed by four washing intervals with MAB, twice at RT for 10min and another two times at 70°C for 30min.

Afterwards embryos were washed three times in PBS⁻w at RT for 10min each and were then pre-incubated in antibody-blocking buffer at 4°C for at least 2hrs. In a second tube the anti-digoxygenin antibody coupled to alkaline phosphatase was diluted 1/10.000 and pre-blocked for the same time. After the two hours of pre-incubation, the blocking buffer was replaced by the blocking solution containing the antibody and the embryos were incubated at 4°C overnight with rocking.

Day 3: On the third day unbound antibody was removed in extensive washing steps and the staining reaction was started. Embryos were rinsed and then washed 5 times for 45min each in PBS⁻w containing 0.1% BSA. The washing in PBS⁻w/BSA was followed by two washing steps in PBS⁻w for 30min each and embryos were then transferred into AP1 buffer, which adjusts the pH of the tissue for the optimal reaction of the alkaline phosphatase. AP1 buffer was changed twice after 10min and then replaced by a 1:1 mixture of AP1 buffer and BM Purple, the substrate for the alkaline phosphatase. The staining process was controlled and stopped by washing in PBS⁻w when the signal had reached a dark blue to violet colour. A gradual methanol series intensified the signal and the embryos were afterwards stored in glycerol at 4°C.

Histological analysis of embryos after *in situ* hybridisation

For histological analysis embryos were equilibrated in embedding medium while the embedding mould was prepared. To form the mould 2ml of embedding medium were mixed shortly but vigorously with 140µl of glutaraldehyde and poured into the two metal brackets arranged to form a square. The mixture was allowed to harden and the equilibrated embryo was transferred and arranged on the surface of the block, excess fluid embedding medium was carefully removed. Another 2ml of embedding medium were mixed with glutaraldehyde and poured into the mould so that the embryo was now sandwiched between two layers of firm embedding mix. The block was then trimmed with a razor blade and glued to a plate. The plate was mounted into the holder of the vibratome and 30µm thick sections were prepared. The sections

were arranged onto glass slides, embedded with mowiol and protected with glass cover slips.

Immunohistochemistry

Whole mount immunohistochemistry was used to detect expression patterns of specific proteins of interest in wild type and cultured rabbit embryos.
Embryos were either used directly after fixation with 4% PFA (4% paraformaldehyde in PBS^-) or were rehydrated from storage in 100% methanol through a graded series of 75, 50 and 25% methanol in PBS^-_T (PBS^- with 0.1% Triton-X 100). Embryos were then washed two times in PBS^-_T for at least 5min and subsequently blocked for 2 hours in CAS-block (1:10 in PBS^-_T) at RT. Afterwards embryos were incubated in 200µl of primary antibody solution (mouse anti-acetylated tubulin, 1:700 in pure CAS-block) for 2 hours at room temperature followed by three washing steps with PBS^-_T for 20min each. In 200µl of secondary antibody solution (anti-mouse IgG-Cy3, 1:250 in pure CAS block) embryos were incubated at 4°C over night again followed by three washing steps in PBS^-_T for 20min each. Afterwards embryos were arranged onto glass slides, embedded with mowiol, protected with glass cover slips and analyzed under a confocal laser scanning microscope (LSM 5 Pascal).

Embryological procedures

All embryos used in this work were either obtained from timed matings of NZW rabbits or from timed incubations of fertilized hen eggs. All steps involving isolation and culture of embryos were carried out under sterile conditions using sterile buffers, media, labware and instruments. Fixation in a solution of 4% paraformaldehyde in PBS^- (4% PFA) was conducted for 1h at RT or at 4°C overnight.

Dissection and storage of embryos

Dissection and fixation of rabbit embryos

After the abdominal cavity of the dead animal had been opened the uterus was removed in whole and transferred to PBS^+ in a 50ml Falcon Tube. If the embryos were to be used for *in vitro* culture the uterus was processed natively. If intended for *in situ* hybridization the uterus was prefixed in 4% paraformaldehyde for 15-20min and washed in PBS^+ afterwards. Uteri from both procedures were transferred into fresh PBS^+ in a large Petri dish (10cm in diameter) where excess fat and mesenteria were removed and the uterus was separated into pieces between the embryo implantation sites. Single parts of the uterus were again transferred into fresh PBS^+ and dissected further under a stereomicroscope using fine tweezers and iridectomy scissors. The bulging uterine tissue opposite of the implantation site was carefully cut and removed until the embryo covering the mucosa became accessible. The embryo together with as much surrounding extraembryonic tissue as possible was cautiously detached from the mucosa and transferred into another dish with fresh PBS^+. From there the embryo was either taken into culture directly (for ring culture) or trimmed further in a circular fashion and used natively for semidry culture or was fixed in 4% paraformaldeyde for *in situ* hybridization.

Dissection and fixation of chick embryos

After incubation for the desired length of time eggs were taken out of the incubator making sure that the embryo stayed on top by not rotating them. Then, eggs were cracked into a 10cm Petri dish using the rim of the dish. If the vitelline membrane stayed intact and the blastoderm was roughly centred on the yolk the preparation proceeded with removing the thick albumen covering the blastoderm with a folded tissue or a plastic pipette. Once an area of vitelline membrane large enough for the filter paper ring was cleared the filter paper ring was placed onto the yolk framing the embryo in the middle. The vitelline membrane was then cut around the filter paper ring using fine scissors. The ring including the embryo attached to the vitelline membrane was gently lifted with tweezers and any remaining yolk was removed from

the ring by stroking the vitelline membrane in a centrifugal fashion with blunt tweezers. The embryo was then transferred into a small Petri dish containing either simple saline or PBS^+ to remove as much yolk as possible by gently flushing the saline over the blastoderm.

Dehydration and storage

If desired, all embryos fixed in 4% PFA could be stored until further utilisation. After fixation had been completed, they were washed three times in PBS for 5min and then dehydrated in an ascending methanol series (25, 50 and 75% methanol in PBS, 2 x 100% methanol). Embryos were stored in 100% methanol at -20°C.

In vitro culture of rabbit embryos

Rabbit embryos intended for *in vitro* culture were dissected as described above, processed for *in vitro* culture and then cultured in a small incubator under humidified air with 5% CO_2 at 38°C until they reached the desired stage.

Preparation of culture dishes

A substratum for the embryo during culture was prepared from 0.5% agarose in PBS^- which had been sterilized by autoclaving and then stored at room temperature. 100µl of remelt agarose were pipetted into small culture dishes (35mm in diameter) and spread out to create a circular mound as flat as possible. Enough culture medium to cover the agarose mound was added to the dishes which were then pre-incubated until further usage.

Preparation of rings

Little plastic rings to place around the embryo onto the extraembryonic tissue during culture were prepared by cutting 3.5ml plastic pipettes using the vibratome. For this purpose the part of the pipette tip providing the appropriate diameter (about 3-5mm) was embedded as described above and cut into 300µm thick sections using very low

speed. The rings were then sterilised by washing with 70% Ethanol and the alcohol was removed by washing thoroughly with sterile water. Afterwards rings were dried on tissue and stored in a box until needed.

Preparation of substance soaked beads

To place proteins or chemical compounds onto the embryo during *in vitro* culture, small beads known form affinity chromatography were used. Affi-Gel Blue Gel beads (for Shh, Cyclopamine and SU5402) or Heparin-coated acrylic beads (for FGF8) were washed three times in 50ml PBS^+ and stored on ice. The lyophilised proteins were reconstituted according to the manufacturer's instructions to a concentration of 1µg/µl and 5µl aliquots were stored at -80°C. Cyclopamine was dissolved in Ethanol at a concentration of 10mM and SU5402 was dissolved in DMSO to a stock solution of 20mM and then aliquoted. Both substances were stored at -20°C. Because SU5402 is likely to deteriorate if exposed to light the substance was kept and handled in the dark whenever possible.

Preparation of modified medium

If it was desirable to have the whole embryo in contact with a drug, the substance was applied directly in the culture medium.

From the 10mM stock solution Cyclopamine was diluted to a concentration of 80µM into 1ml portions of culture medium directly before use. SU5402 was diluted from the 20mM stock solution to a concentration of 60µM into culture medium and 1.5% methyl cellulose were dissolved in culture medium by stirring overnight.

Placement of embryos onto agarose mounds

Single embryos prepared from native uteri were carefully transferred into a medium filled culture dish using a plastic pipette. With fine tungsten needles the embryo was gently pulled up the agarose mound and spread out, ectoderm down, on top of the mound. Surplus medium was now removed with a pulled out glass pipette and the fluid level was adjusted so that it just reached the extraembryonic tissue. In this way, the embryo was held in place by the surface tension of the medium and also wetted

by a thin liquid film in standard, semi-dry cultures. For ring cultures a plastic ring of the appropriate size was selected and carefully put onto the extraembryonic tissue framing the embryo. If necessary the extraembryonic tissue was wrapped around the ring to fix the embryo properly and to provide more tension. Then the ring was filled with a drop of medium to supply the embryo with a higher liquid film than in standard cultures.
When embryos should be cultured in modified medium, dishes were taken from the incubator, the pre-incubated medium was removed and replaced by fresh modified medium. The embryo was then transferred directly into the modified medium and placed onto the agarose mound as described above. The only exception from this routine were the experiments with 1.5% methylcellulose in culture medium where the embryo was placed first onto the mound, the pre-incubated medium was then completely removed and replaced by medium containing 1.5% methylcellulose.

Implantation of substance soaked beads

Using a sharpened tungsten needle a small lesion was scraped into the embryo at the respective site of bead implantation. With a little hook bent into the tip of a tungsten needle, a bead was picked from the droplet in which it has been incubated. It was placed onto the embryo and carefully pushed into place so that it came to lie between ecto- and endoderm. After positioning the bead, the ring was placed and filled with medium as described above and the embryo was put in the incubator and cultured to the desired stage.

Fixation of cultured embryos

After culture was completed, the medium was aspirated and replaced with 4% PFA which was filled in high enough to lift the embryo off the agarose mound and let the tissue float on the surface of the fixative. Embryos were either fixed for one hour at room temperature or at 4°C overnight. Rings were removed when fixation was completed and embryos were then prepared for storage as described above.

In vitro culture of chick embryos

Chick embryos intended for *in vitro* culture were dissected as described above. After removing as much yolk as possible with simple saline or PBS^+, excess fluid was absorbed by dabbing an edge of the filter paper ring on a piece of tissue paper. This prevents the collection of excess liquid in the shallow well above the embryo during culture. The filter paper ring with the embryo was then carefully placed onto an agarose-albumen culture dish with the blastoderm ventral side up avoiding to trap any air bubbles between the embryo and the substratum. The embryos were then put into the small incubator either natively or a substance soaked bead was implanted as described above and cultured until they reached the desired stage.

Preparation of filter paper rings and culture dishes

Rings with an outer diameter of 3cm and an inner diameter of 1.3cm were cut out of chromatography paper.

For culture dishes 60 ml of simple saline with 0.6% agarose were heated until the agarose was melted. Also 60ml thin albumen of unincubated eggs were collected and both liquids were equilibrated at 49°C. Then the liquids were mixed thoroughly and 5U/ml penicillin/streptomycin were added. Using a 10ml pipette 2.5ml of the mixture was aliquoted into each 35mm culture dish without introducing any bubbles. After replacing the lids the dishes were left to dry at room temperature for several hours or overnight and then stored in an airtight container at 4°C or up to 2 weeks.

Structural analysis of cultured embryos

Scanning electron microscopy

Embryos cultured either with the standard method or the ring method were gently rinsed with culture medium to remove cell debris that had accumulated during the incubation period and were then immersion fixed with a mixture of 4% PFA and 2.5%

glutaraldehyde for 1h at room temperature or at 4°C overnight. The specimens were washed three times for 10min in 0.1M phosphate buffer (PB) and were then postfixed for 1h in 1% OsO_4 in 0.1 M PB at 4°C. After another three times of washing in PB for 10min the embryos were gradually dehydrated in an ethanol series (15% in PB, 30% in PB, 50% in PB and DDW, 70% in DDW, 90% in DDW and 2 x 100% ethanol) and stored in 100% ethanol at 4°C until submitted to the drying procedure. Critical point drying was performed using CO_2 as a drying agent. Afterwards embryos were sputtered with gold and analysed under a LEO DSM 940A.

Analysis of cilia-driven leftward flow in rabbit embryos

Cilia-driven leftward fluid flow was analyzed in wild type, standard- or ring-cultured embryos. Therefore embryos were dissected and processed as described above. Cultured embryos were gently rinsed with culture medium to remove cell debris that had accumulated during the incubation period prior to analysis.

Fluorescence microscopic analysis

For fluorescence microscopic analysis embryos were transferred into culture medium containing 200nm big fluorescent latex beads (FluoSpheres®) in a concentration of 1:2500. On a glass slide a rectangle was formed using Vaseline. The embryo was transferred into the rectangle with a drop of medium using a plastic pipette, arranged with its ventral side up and then covered with glass cover slips. Due to the Vaseline the distance between glass slide and cover slip was adjustable. After excitation with UV light (Osram HBO mercury vapour lamp with aspherical collector, Zeiss) at a wavelength of 395/475nm the emitted light (509nm) of the fluorescent beads was recorded with the help of a CCD camera (AxioCam HSc, Zeiss) and the axiovision software 4.6 (Zeiss). Time-lapse movies were 500 frames long with 2 frames/s.

Semi-automated processing of raw data

Raw data obtained with the axiovision software was further processed using the open source programme ImageJ (http://rsb.info.nih.gov/ij/) and the plugin “ParticleTracker” (Sbalzarini and Koumoutsakos; J. Struct. Biol., 2005) as well as a custom-made macro in statistical R (http://www.r-project.org/; Hornik, 2008) based on a macro developed by Weber, 2006. The obtained films and corresponding bright-field images were exported as .tif files and loaded in ImageJ. Here, images were rotated arbitrarily so that the PNC was viewed with anterior to the top. Then images were cropped to a standard size of 360x432 pixels and, by running the film, a mask was defined to exclude regions where backflow was filmed. After running the plugin “Particle tracker” the obtained .txt file was saved and processed further with the macro. The custom-made statistical R macro included the following operations:

Step 1: for each trail a bezier fit curve was calculated with an iteration level of 10 (i.e. 10 points per curve).

Step 2: for flow calculation only trails were selected that 1) appeared in more than 10 consecutive frames to eliminate artefacts of the “Particle tracker” and 2) showed a rho value of grater than 0.6 (empirically determined). In this context rho represents the mean resultant length of a vector for the significance of the mean direction calculated with the Rayleigh test of uniformity based on the bezier curve of the trails. Rho=0 represents completely random direction (points of bezier curve are distributed randomly), rho=1 represents exactly straight trails aiming in the same direction (points of bezier curve are distributed in a straight line). With the remainder of trails again a Rayleigh test was performed to calculate the rho value for the whole film. The result was also graphically depicted in a windrose histogram subdivided into groups of 45°.

Visualisation: to visualise direction and movement, the trails were differentially coloured over time from t=0s (green) via t=12.5s (yellow) to t=25s (red) and then merged into one frame yielding a Gradient Time Trail (GTT). In the case of a movie the next frame comprised the 51 consecutive frames covering t=0.5s to t=25.5s.

Buffers, solutions and media

For bacteria culture

Super Optimal Catabolite repression medium (S.O.C.)

0.5% Yeast extract
2.0% Tryptone
10mM NaCl
2.5mM KCl
10mM $MgCl_2$
10mM $MgSO_4$
20mM Glucose
autoclave

Lysogeny Broth (LB) medium

1%Tryptone
1% NaCl
0.5% Yeast extract
adjust pH to 7.0, autoclave

LB agar

1% Tryptone
1% NaCl
0.5% Yeast extract
adjust pH to 7.0, add 15g/l agar before autoclaving

For DNA preparation

P1

50mM TRIS HCl
10mM EDTA pH 8
add RNaseA (DNase free) to a final concentration of 100µg/ml

P2

0.2M NaOH
1% SDS

P3

3M Potassium acetate, adjust pH to 5.5 with glacial acetic acid

For *in situ* hybridisation

Phosphate buffered saline 10x (PBS^-, 1l)

80g NaCl
2g KCl
14.4g Na_2HPO_4
2.4g KH_2PO_4
800ml DDW
adjust pH to 7.4, add DDW to 1l, autoclave
PBS_w = PBS with 0.1% Tween-20

Hybridisation solution (1l)

10g Boehringer Block
500ml Formamide
250ml SSC 20x
heat to 65°C for 1h
120ml DDW
100ml Torula RNA (10mg/ml in DDW, filtered)
2ml Heparin (50mg/ml in 1x SSC pH 7)
5ml 20% Tween-20
10ml 10% CHAPS
10ml 0.5M EDTA

Sodium Sodium Citrate Buffer 20x (SSC, 1l)

175.3g NaCl
88.2g Sodium Citrate
800ml DDW
adjust pH to 7.0, add DDW to 1l, autoclave

Maleic Acid Buffer 5x (MAB, 1l)

58.05g (100mM) Maleic Acid
43.83g (150mM) NaCl
800ml DDW
adjust pH to 7.5 with 10N NaOH, add DDW to 1l, autoclave

Antibody Blocking Buffer

1% Boehringer Block
dissolve in PBS at 70°C, vortexing frequently
10% Goat Serum (heat inactivated 30min 56°)
0.1% Tween-20
filter

Alkaline Phosphatase Buffer (AP1, 1l)

100ml 1M TRIS pH 9.5
20ml 5M NaCl
50ml 1M MgCl
add DDW to 1l

For electron microscopy

Sörensen Phosphate Buffer

Stock solution A: 0.2M NaH_2PO_4
Stock solution B: 0.2M Na_2HPO_4
For 0.1M pH 7.4: 19ml a, 81ml B, 100ml DDW

For other applications

Medium for rabbit embryo *in vitro* culture

F-10 Nutrient Mixture with L-Glutamine
20% Fetal Bovine Serum (heat inactivated 30min 56°C)
2% Penicillin/Streptomycin

Simple Saline for dissection of chick embryos (1l)

7.19g NaCl
add DDW to 1l, autoclave

Embedding medium for vibratome sections

2.2g Gelatine
135g Bovine Serum Albumin
90g Saccharose
dissolve in 450ml PBS

Mowiol (Mounting medium)

96g Mowiol 488
24g Glycerol
24ml DDW
stir for 2h, then add
48ml TRIS 0.2M pH 8.5
stir for 20min at 50°C
centrifuge for 15min at 5000rpm, keep supernatant and store at 4°C

Tris Acetate EDTA Electrophoresis Buffer 50x (TAE, 1l)

242g Tris base
57.1ml Glacial acetic acid
100ml 0.5M EDTA pH 8.0
add DDW to 1l, adjust pH to 8.5

Sources of supply

Chemicals and labware:

Affi-Gel Blue Gel	BIO RAD, Munich
Agar	Applichem, Darmstadt
Agarose	Roth, Karlsruhe
Ampicillin	Applichem, Darmstadt
Boehringer Block	Roche, Mannheim
Bovine serum albumin	Applichem, Darmstadt
BM Purple	Roche, Mannheim
CAS-Block	Zymed (Invitrogen), Karlsruhe
Chloroform	Merck, Darmstadt
CHAPS	Sigma, Schnelldorf
Cyclopamine	Biomol, Hamburg
Dig-Mix	Roche, Mannheim
Disodium hydrogen phosphate	Applichem, Darmstadt
DTT	Promega, Mannheim
DMSO	Roth, Karlsruhe
Deoxynucleotide triphosphates (dNTPs)	Promega, Mannheim
EDTA	Roth, Karlsruhe
Ethanol	Roth, Karlsruhe
Ethidiumbromide	Roth, Karlsruhe
F10 medium	Gibco (Invitrogen), Karlsruhe
Falcon Tubes (15ml, 50ml)	VWR, Darmstadt

Fetal bovine serum	Sigma, Schnelldorf
Filter (chromatography) paper	Schleicher & Schuell, Dassel
FluoSpheres® (200nm)	Invitrogen, Karlsruhe
Formamide	Roth, Karlsruhe
Gelatine	Roth, Karlsruhe
Glacial acetic acid	Applichem, Darmstadt
Glass slides, Glass coverslips	Roth, Karlsruhe
Glutaraldehyde	Applichem, Darmstadt
Glucose	Applichem, Darmstadt
Glycerol	Roth, Karlsruhe
Glycine	Applichem, Darmstadt
Goat serum	Sigma, Schnelldorf
HCl (37%)	Merck, Darmstadt
Heparin	Sigma, Schnelldorf
Heparin-Acrylic beads	Sigma, Schnelldorf
Iridectomy scissors	Fine Science Tools, Heidelberg
Lithium chloride	Serva, Heidelberg
Loading buffer	Applichem, Darmstadt
Maleic acid	Roth, Karlsruhe
Magnesium chloride	Roth, Karlsruhe
Magnesium sulfate	Applichem, Darmstadt
Methanol	Roth, Karlsruhe
Methylcellulose	Sigma, Schnelldorf
Microcentrifuge tubes, PCR tubes	Sarstedt, Nümbrecht
Multi-well plates	Greiner, Frickenhausen
NaOH	Merck, Darmstadt
Oligonucleotides	Operon, Cologne
Osmium tetroxide	Plano, Wetzlar
Parafilm	Roth, Karlsruhe
Paraformaldehyde	Applichem, Darmstadt
PBS^{+} (10x)	Gibco (Invitrogen), Karlsruhe

Penicillin/Streptomycin	Gibco (Invitrogen), Karlsruhe
Petri dishes	Greiner, Frickenhausen
Plastic pipettes	Roth, Karlsruhe
Potassium acetate	Roth, Karlsruhe
Potassium chloride	Merck, Darmstadt
Potassium dihydorgen phosphate	Merck, Darmstadt
2-Propanol	Roth, Karlsruhe
Proteinase K	Roth, Karlsruhe
Random hexamers	Promega, Mannheim
RNAse A	Roth, Karlsruhe
RNAsin	Promega, Mannheim
Saccharose	Applichem, Darmstadt
Sodium acetate	Roth, Karlsruhe
Sodium chloride	Roth, Karlsruhe
Sodium dihydrogen phosphate	Applichem, Darmstadt
Sodium dodecyl sufate (SDS)	Roth, Karlsruhe
Sodium hydroxide	Applichem, Darmstadt
SU5402	Calbiochem, Bad Soden
T61	Hoechst, Frankfurt
Tissue culture dishes	Greiner, Frickenhausen
Torula RNA	Sigma, Schnelldorf
TRIS base	Applichem, Darmstadt
TRIS HCl	Applichem, Darmstadt
Triton-X 100	Serva, Heidelberg
Tryptone	Applichem, Darmstadt
Tungsten wire	Plano, Wetzlar
Tween-20	Applichem, Darmstadt
Tweezers (#3, #5)	Fine Science Tools, Heidelberg
Vaseline	MainoPharm, Frankfurt
X-Gal	Roche, Mannheim
Yeast extract	Roth, Karlsruhe

Kits:

TOPO TA Cloning Kit	Invitrogen, Karlsruhe
pGEM-T Easy Vector System	Promega, Mannheim
PureYield Plasmid Midiprep System	Promega, Mannheim
PeqGOLD TriPure™	Peqlab, Erlangen

Proteins and Antibodies:

Anti-mouse IgG-Cy3	Sigma, Schnelldorf
Anti-digoxigenin AP	Roche, Mannheim
Modifying enzymes and buffers	Promega, Mannheim
Mouse anti-acetylated tubulin	Sigma, Schnelldorf
Recombinant human SHH	R&D Systems, Wiesbaden
Recombinant mouse FGF8b	R&D Systems, Wiesbaden
Restriction enzymes and buffers	Promega, Mannheim

Animals:

Rabbits (New Zealand White)	Haussler, Schwäbisch Hall
Fertilized hen eggs	Eierhof Müller, Großbottwar

Special Hardware:

Critical point dryer CPD 030	Balzers, Austria
Heat Sterilizer	Fine Science Tools, Heidelberg
Incubator Gasboy C42	Labotect, Göttingen
LEO DSM 940A	Zeiss, Oberkochen
LSM 5 Pascal	Zeiss, Oberkochen
Stereo microscope, Stemi 2000 C	Zeiss, Oberkochen
Sputter coater SCD 050	Balzers, Austria
Vibratome	Leica, Bensheim
Eggincubator, KMB2	Ehret, Emmendingen

Supplement

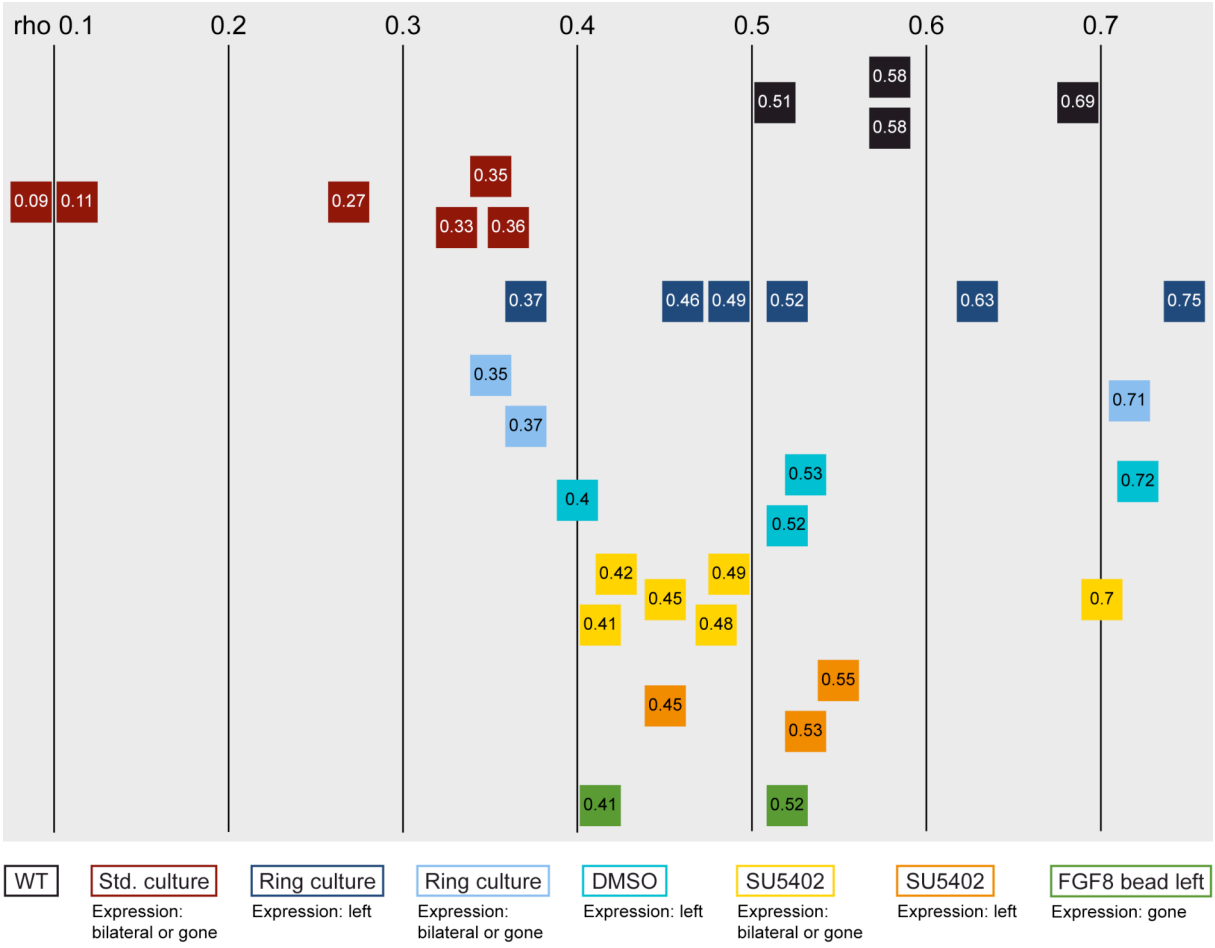

Supplementary Fig. 1 Overview of rho values (quality) of all flow films analyzed in this study. Every square represents one embryo with its individual rho value stated. Wild type (WT) embryos examined ranged from the 2-3 somite stage to 4 somites and are depicted in black. All embryos cultured and filmed afterwards had 3-5 somites when filmed. Standard-cultured (Std. culture) embryos are shown in red and displayed bilateral or no marker gene expression after *in vitro* culture. Untreated ring-cultured embryos with left-sided expression are shown in blue and with altered expression in light blue. Rho values of films of ring-cultured embryos treated with DMSO and left-sided marker gene expression are depicted in turquoise. Ring-cultured embryos incubated with SU5402 are shown in yellow and orange, showing altered or normal left-sided expression, respectively. Films of ring-cultured embryos that received an FGF8 loaded bead and lacked marker gene expression are depicted in green.

A

Ihh

```
1   GCC GAC CGC CTC ATG ACC CAG CGC TGC AAG GAC CGC CTG AAC TCG CTG GCC ATC TCC GTG  60
1    A   D   R   L   M   T   Q   R   C   K   D   R   L   N   S   L   A   I   S   V   20

61  ATG AAC CAG TGG CCC GGC GTG AAG CTG CGG GTG ACT GAA GGC TGG GAC GAG GAC GGC CAC 120
21   M   N   Q   W   P   G   V   K   L   R   V   T   E   G   W   D   E   D   G   H   40

121 CAC TCG GAG GAG TCC TTG CAT TAT GAG GGT CGC GCA GTG GAC ATC ACC ACG TCC GAC CGT 180
41   H   S   E   E   S   L   H   Y   E   G   R   A   V   D   I   T   T   S   D   R   60

181 GAC CGC AAT AAG TAC GGA CTG CTG GCG CGC TTG GCA GTG GAG GCC GGC TTC GAC TGG GTG 240
61   D   R   N   K   Y   G   L   L   A   R   L   A   V   E   A   G   F   D   W   V   80

241 TAT TAC GAG TCC AAG GCC CAC GTG CAT TGC TCG GTC AAG TCC GAG CAC TCG GCC GCA GCC 300
81   Y   Y   E   S   K   A   H   V   H   C   S   V   K   S   E   H   S   A   A   A  100

301 AAG ACT GGT GGC TGC TTC CCC GCC GGA GCG CAG GTG CGC CTG GAG AGT GGC GCA CGC GTG 360
101  K   T   G   G   C   F   P   A   G   A   Q   V   R   L   E   S   G   A   R   V  120

361 GCC ATG TCA GCC GTG AGG CCG GGA GAC CGG GTG CTA GCC ATG GGG GAG GAC GGA AAC CCC 420
121  A   M   S   A   V   R   P   G   D   R   V   L   A   M   G   E   D   G   N   P  140

421 ACC TTC AGC GAC GTA CTC ATT TTC CTG GAC CGC GAG CCT GAC AGG CTG AGG GCC TTC CAG 480
141  T   F   S   D   V   L   I   F   L   D   R   E   P   D   R   L   R   A   F   Q  160

481 GTC ATC GAG ACC CAA GAC CCT CCA CGG CGC CTG GCG CTC ACC CCG GCC CAC CTG CTC TTC 540
161  V   I   E   T   Q   D   P   P   R   R   L   A   L   T   P   A   H   L   L   F  180

541 ACG GCC GAC AAT CGC ACA GAG ACA GCA GCC CGC TTC CGG GCC ACG TTC GCC AGC CAC GTG 600
181  T   A   D   N   R   T   E   T   A   A   R   F   R   A   T   F   A   S   H   V  200

601 CAG CCT GGC CAG TAC GTG CTG GTG GCC GGG GTG CCG GGC CTG CAG CCT GCC CGA GTG GCG 660
201  Q   P   G   Q   Y   V   L   V   A   G   V   P   G   L   Q   P   A   R   V   A  220

661 GCT GTG TCC ACC CAC GTG GCC CTC GGG GCC TAC GCC CCC CTC ACG AGG CAC GGG ACG CTG 720
221  A   V   S   T   H   V   A   L   G   A   Y   A   P   L   T   R   H   G   T   L  240

721 GTG GTA GAA GAT GTG GTC GCT TCC TGC TTC GCG GCT GTG GCT GAC CAC CGG CTG GCT CAG 780
241  V   V   E   D   V   V   A   S   C   F   A   A   V   A   D   H   R   L   A   Q  260

781 TTG GCC TTC TGG CCC C                                                        796
261  L   A   F   W   P                                                            265
```

B

Dhh

```
1    GC CCG AGC TGC GGG CCG GGC CGG GGA CCA GTT GGC CGG CGC CGC TAC GTG CGC AAG CAG  59
1        P   S   C   G   P   G   R   G   P   V   G   R   R   R   Y   V   R   K   Q  19

60  CTC GTG CCG CTC CTC TAC AAG CAA TTC GTG CCC AGC ATG CCT GAA CGG ACC CTG GGC GCC 119
20   L   V   P   L   L   Y   K   Q   F   V   P   S   M   P   E   R   T   L   G   A  39

120 AGT GGG CCG GCC GAG GGG AGG GTG GCC AGG GGC TCT GAG CGC TTC CGG GAC CTG GTG CCC 179
40   S   G   P   A   E   G   R   V   A   R   G   S   E   R   F   R   D   L   V   P  59

180 AAC TAC AAC CCC GAC ATC ATC TTC AAG GAT GAA GAG AAC ACT GGC GCA GAC CGC CTG ATG 239
60   N   Y   N   P   D   I   I   F   K   D   E   E   N   T   G   A   D   R   L   M  79

240 ACA GAG CGC TGC AAG GAG CGC GTG AAT GCT CTG GCC ATT GCT GTG ATG AAC ATG TGG CCC 299
80   T   E   R   C   K   E   R   V   N   A   L   A   I   A   V   M   N   M   W   P  99

300 GGA GTG CGC CTC CGG GTG ACG GAG GGC TGG GAC GAG GAC GGC CAC CAC GCT CAG GAC TCG 359
100  G   V   R   L   R   V   T   E   G   W   D   E   D   G   H   H   A   Q   D   S 119

360 CTG CAC TAC GAA GGC AGG GCC CTG GAC ATT ACC ACC TCC GAC CGC GAT CGC AAT AAG TAC 419
120  L   H   Y   E   G   R   A   L   D   I   T   T   S   D   R   D   R   N   K   Y 139

420 GGG CTG CTG GCG CGC CTG GCC GTG GAG GCC GGC TTC GAC TGG GTC TAC TAT GAG TCT CGC 479
140  G   L   L   A   R   L   A   V   E   A   G   F   D   W   V   Y   Y   E   S   R 159

480 AAC CAC GTC CAC GTG TCG GTC AAA GCT GAT AAC TCC CTG GCC GTG AGG GCA GGT GGT TGC 539
160  N   H   V   H   V   S   V   K   A   D   N   S   L   A   V   R   A   G   G   C 179

540 TTT CCG GGA AAC GCT ACG GTG CGC CTG CAG AGC GGC GAG CGG AAG GGC CTG CGG GAG CTG 599
180  F   P   G   N   A   T   V   R   L   Q   S   G   E   R   K   G   L   R   E   L 199

600 CAT CGC GGA GAC TGG GTT CTG GCG GCC GAT GCG GCG GGC CGG GTG GTG CCC ACG CCC GTG 659
200  H   R   G   D   W   V   L   A   A   D   A   A   G   R   V   V   P   T   P   V 219

660 CTG CTC TTC CTG GAC CGG GAC TTG CAG CGC CGG GCC TCC TTC GTG GCT GTG GAG ACC GAG 719
220  L   L   F   L   D   R   D   L   Q   R   R   A   S   F   V   A   V   E   T   E 239

720 CGG CCT CCG CGC AAA CTG CTG CTC ACG CCC TGG CAC CTG GTG TTC GCT GCT CGC GGG CCG 779
240  R   P   P   R   K   L   L   L   T   P   W   H   L   V   F   A   A   R   G   P 259

780 GCT CCC GAG CCG GGG GAC TTT GCA CCG GTG TTC GCG CGC C                          819
260  A   P   E   P   G   D   F   A   P   V   F   A   R                          272
```

C

Smo

```
1    GC TGG TAC GAG GAC GTG GAG GGC TGC GGG ATC CAG TGT CAG AAC CCG CTC TAC ACC GAA  59
1        W   Y   E   D   V   E   G   C   G   I   Q   C   Q   N   P   L   Y   T   E   19

60  GCC GAA CAC CAG GAC ATG CAC AGC TAC ATC GCC GCC TTC GGC GCC ATC ACA GGC CTC TGC 119
20   A   E   H   Q   D   M   H   S   Y   I   A   A   F   G   A   I   T   G   L   C  39

120 ACG CTC TTC ACC CTG GCC ACG TTT GTG GCT GAC TGG CGG AAC TCG AAT CGC TAC CCT GCT 179
40   T   L   F   T   L   A   T   F   V   A   D   W   R   N   S   N   R   Y   P   A  59

180 GTC ATC CTC TTC TAT GTC AAC GCA TGT TTC TTC GTG GGC AGC ATC GGC TGG CTG GCC CAG 239
60   V   I   L   F   Y   V   N   A   C   F   F   V   G   S   I   G   W   L   A   Q  79

240 TTC ATG GAC GGG GCC CGC CGG GAG ATC GTC TGT CGG GCA GAT GGC ACC ATG AGG CTG GGG 299
80   F   M   D   G   A   R   R   E   I   V   C   R   A   D   G   T   M   R   L   G  99

300 GAG CCC ACC TCC AAT GAG ACC CTG TCC TGC GTC ATC ATC TTT GTC ATC GTG TAC TAT GCC 359
100  E   P   T   S   N   E   T   L   S   C   V   I   I   F   V   I   V   Y   Y   A 119

360 CTG ATG GCT GGC GTG GTC TGG TTT GTG GTC CTC ACT TAC GCC TGG CAC GCC TCC TTC AAA 419
120  L   M   A   G   V   V   W   F   V   V   L   T   Y   A   W   H   A   S   F   K 139

420 GCG CTG GGC ACC ACC TAC CAG CCT CTC TCG GGC AAG ACC TCC TAC TTC CAC CTG CTG ACG 479
140  A   L   G   T   T   Y   Q   P   L   S   G   K   T   S   Y   F   H   L   L   T 159

480 TGG TCC CTG CCC TTC GTC CTC ACC GTG GCC ATC CTT GCT GTG GCT CAG GTG GAC GGG GAC 539
160  W   S   L   P   F   V   L   T   V   A   I   L   A   V   A   Q   V   D   G   D 179

540 TCT GTG AGC GGC ATC TGT TTC GTG GGC TAC AAG AAC TAC CGA TAC CGT GCC GGC TTC GTG 599
180  S   V   S   G   I   C   F   V   G   Y   K   N   Y   R   Y   R   A   G   F   V 199

600 CTG GCC CCC ATC GGC CTG GTG CTG ATC GTG GGA GGC TAC TTC CTC ATC CGA GGA GTC ATG 659
200  L   A   P   I   G   L   V   L   I   V   G   G   Y   F   L   I   R   G   V   M 219

660 ACT TTG TTC TCC ATC AAG AGC AAC CAC CCC GGG CTG CTG AGC GAG AAG GCG GCG AGC AAG 719
220  T   L   F   S   I   K   S   N   H   P   G   L   L   S   E   K   A   A   S   K 239

720 ATC AAC GAG ACC ATG CTA CGC CTG GGC ATT TTC GGT TTC CTG GCT TTT GGC TTC GTG CTC 779
240  I   N   E   T   M   L   R   L   G   I   F   G   F   L   A   F   G   F   V   L 259

780 ATT ACC TTC AGC TGC CAC TTC TAC GAC TTC TTC AAC CAG GCT GAG TGG GAG CGC AGC TTC 839
260  I   T   F   S   C   H   F   Y   D   F   F   N   Q   A   E   W   E   R   S   F 279

840 CGG GAC TAT GTG CTG TGC CAG GCC AAT GTG ACC ATC GGG CTG CCC ACC AAG AAG CCC ATC 899
280  R   D   Y   V   L   C   Q   A   N   V   T   I   G   L   P   T   K   K   P   I 299

900 CCC GAC TGC GAG ATC AAG AAT CGC CCC AGC CTG CTG GTG GAG AAG ATC AAC CTG TTT GCC 959
300  P   D   C   E   I   K   N   R   P   S   L   L   V   E   K   I   N   L   F   A 319

960 ACG TTC GGA ACT GGC ATT TCC ATG AGC ACC TGG GTC TGG ACC AAG GCC AC            1009
320  T   F   G   T   G   I   S   M   S   T   W   V   W   T   K   A               335
```

D

Hip

```
1    CT TGC CGA GGC CAT ATT CCA GGT TTC CTT CAA ACA ACT GCT GAT GAG TTT TGC TTT TAC  59
1        C   R   G   H   I   P   G   F   L   Q   T   T   A   D   E   F   C   F   Y   19

60  TAT GCA AGA AAA GAT GGT GGG CTG TGC TTT CCA GAT TTT CCA AGA AAA CAA GTC AGA GGA 119
20   Y   A   R   K   D   G   G   L   C   F   P   D   F   P   R   K   Q   V   R   G   39

120 CCA GCA TCT AAC TAC TTG GAC CAG ATG GAA GAA TAT GAC AAA GTG GAA GAG ATC AGC AGA 179
40   P   A   S   N   Y   L   D   Q   M   E   E   Y   D   K   V   E   E   I   S   R   59

180 AAG CAC AAA CAC AAC TGC TTC TGC ATT CAG GAG GTT GTG AGC GGG CTG CGG CAG CCT GTT 239
60   K   H   K   H   N   C   F   C   I   Q   E   V   V   S   G   L   R   Q   P   V   79

240 GGT GCC CTG CAC AGC GGG GAC GGC TCG CAC CGC CTC TTC ATT CTG GAA AGG GAA GGC TAC 299
80   G   A   L   H   S   G   D   G   S   H   R   L   F   I   L   E   R   E   G   Y   99

300 GTG AAG ATA CTT ACC CCT GAA GGA GAC ATT TTC AAG GAG CCT TAT TTG GAC ATT CAC AAA 359
100  V   K   I   L   T   P   E   G   D   I   F   K   E   P   Y   L   D   I   H   K  119

360 CTT GTT CAA AGT GGA ATA AAG GGA GGA GAT GAA AGA GGA CTG CTA AGC CTC GCA TTC CAT 419
120  L   V   Q   S   G   I   K   G   G   D   E   R   G   L   L   S   L   A   F   H  139

420 CCC AAT TAC AAG AAA AAT GGA AAG CTC TAT GTG TCT TAT ACC ACC AAC CAA GAA CGG TGG 479
140  P   N   Y   K   K   N   G   K   L   Y   V   S   Y   T   T   N   Q   E   R   W  159

480 GCT ATC GGG CCT CAT GAC CAC ATT CTC AGG GTT GTG GAA TAC ACA GTA TCC AG          532
160  A   I   G   P   H   D   H   I   L   R   V   V   E   Y   T   V   S              176
```

E

Gdf1

```
1 C CGG AAA CAT CGT GCG CCA CAT CCC GAC CGC GGT GCG CCT GTC CGC GCC GCC GGC CCC GCC  61
1    R   K   H   R   A   P   H   P   D   R   G   A   P   V   R   A   A   G   P   A   20

62  CCG GCC GCC GGC CCG TGC CCC GGG TGG ACC GCG CTC TTC GAC CTG GCG GCC GTG GAG CCC 121
21   P   A   A   G   P   C   P   G   W   T   A   L   F   D   L   A   A   V   E   P   40

122 GCC GAG CGC CCG AGC CGG GCC CGC CTG GAG CTG CGC TTC GCG GCG GCC GAG ACC CCC GCG 181
41   A   E   R   P   S   R   A   R   L   E   L   R   F   A   A   A   E   T   P   A   60

182 GAC GGC TGG GAG CTG AGC GTG GCG CGC GCG GGG GAC GCG GCG GGC CCC GGG CCG GTG CTG 241
61   D   G   W   E   L   S   V   A   R   A   G   D   A   A   G   P   G   P   V   L   80

242 CTG CGC CAG GAA GTG GCG GCC CTC GAC CGG CCG GTG CGC GCC GAG CTG CTG GGC GTC GCC 301
81   L   R   Q   E   V   A   A   L   D   R   P   V   R   A   E   L   L   G   V   A  100

302 TGG GCC CGC AAC GCC TCG GCG CCC CGC AGC CTC CGC CTG GCG CTG GCG CTG CGG CCC CGG 361
101  W   A   R   N   A   S   A   P   R   S   L   R   L   A   L   A   L   R   P   R  120

362 GCC CCC GCC GCC TGC GCG CGC CTG GCC GAA GCC TCG CTG CTG CTG GTG ACC CTG GAC CCG 421
121  A   P   A   A   C   A   R   L   A   E   A   S   L   L   L   V   T   L   D   P  140

422 CGC CTC TGC CGG CCC CGC ACG CGG CGC GAG GCG GAG CCC GTG GTG GGC GGC GCC GGG GCG 481
141  R   L   C   R   P   R   T   R   R   E   A   E   P   V   V   G   G   A   G   A  160

482 TGT CGC GCG CGG CGG CTC TAC GTG AGC TTC CGC GAG GTG GGC TGG CAC CGC TGG GTC ATC 541
161  C   R   A   R   R   L   Y   V   S   F   R   E   V   G   W   H   R   W   V   I  180

542 GCG CCG CGC GGC TTC CTG GCC AAC TAC TGC CAG GGC GGC TGC GGG CTG CCC GCC GCG CTG 601
181  A   P   R   G   F   L   A   N   Y   C   Q   G   G   C   G   L   P   A   A   L  200

602 CCC GCG CCC GGG GGC CCG CCC GTG CTC AAC CAC GCT GTG CTG CGC GCG CTC ATG CAC GC  660
201  P   A   P   G   G   P   P   V   L   N   H   A   V   L   R   A   L   M   H      219
```

Supplementary Fig. 2 Nucleotide- and deduced amino acid-sequence of rabbit Hh-signalling marker gene-fragments cloned by RT-PCR. (**A**) 796bp fragment of *Ihh*, the conserved N-terminal signalling domain is underlined. (**B**) 819bp fragment of *Dhh*. the conserved N-terminal signalling domain is underlined. (**C**) 1009bp fragment of *Smo*, the membrane spanning Frizzled/Smoothened domain is underlined. (**D**) 532bp fragment of *Hip*. (**E**) 660bp fragment of *Gdf1*, the TGFβ domain is underlined.

References

Adachi H, Saijoh Y, Mochida K, Ohishi S, Hashiguchi H, Hirao A, Hamada H. 1999. **Determination of left/right asymmetric expression of nodal by a left side-specific enhancer with sequence similarity to a lefty-2 enhancer**. Genes Dev 13:1589-1600.

Afzelius BA. 1976. **A human syndrome caused by immotile cilia**. Science 193: 317–319.

Aglyamova GV, Agarwala S. 2007. **Gene expression analysis of the hedgehog signaling cascade in the chick midbrain and spinal cord**. Dev Dyn. 236(5): 1363-73.

Alcedo J, Ayzenzon M, Vonohlen T, Noll M, Hooper J. 1996. **The Drosophila smoothened gene encodes a 7-pass membrane-protein, a putative receptor for the hedgehog signal**. Cell 86: 221–232.

Amack JD, Yost HJ. 2004. **The T box transcription factor no tail in ciliated cells controls zebrafish left-right asymmetry**. Curr Biol 14(8): 685-90.

Amack JD, Wang X, Yost HJ. 2007. **Two T-box genes play independent and cooperative roles to regulate morphogenesis of ciliated Kupffer's vesicle in zebrafish**. Dev Biol 310(2): 196-210.

Beales PL. 2005. **Lifting the lid on Pandora's box: the Bardet-Biedl sydrome**. Curr Opin Genet Dev 15(3): 315-23

Beckers A, Alten L, Viebahn C, Andre P, Gossler A. 2007. **The mouse homeobox gene Noto regulates node morphogenesis, notochordal ciliogenesis, and left-right patterning**. PNAS 104(40): 15765–15770

Beddington RS, Rashbass P, Wilson V. 1992. **Brachyury--a gene affecting mouse gastrulation and early organogenesis**. Dev Suppl: 157-65.

Bitgood MJ, McMahon AP. 1995. **Hedgehog and Bmp genes are coexpressed at many diverse sites of cell-cell interaction in the mouse embryo**. Dev Biol 172: 126–138.

Bitgood M, Shen L, McMahon A. 1996. **Sertoli-cell signaling by Desert hedgehog regulates the male germline**. Curr Biol 6: 298–304.

Blum M, Andre P, Muders K, Schweickert A, Fischer A, Bitzer E, Bogusch S, Beyer T, van Straaten HWM, Viebahn C. 2007. **Ciliation and gene expression distinguish between node and posterior notochord in the mammalian embryo**. Differentiation 75(2):133-46

Blum M, Weber T, Beyer T, Vick P. **Evolution of cilia-driven leftward flow**. Sem Cell Dev Biol: under review

Boettger T, Wittler L, Kessel M. 1999. **FGF8 functions in the specification of the right body side of the chick**. Curr Biol 9: 277-280

Bonnafe E, Touka M, AitLounis A, Baas D, Barras E, Ucla C, Moreau A, Flamant F, Dubruille R, Couble P, Collignon J, Durand B, Reith W. 2004. **The transcription factor RFX3 directs nodal cilium development and left-right asymmetry specification**. Mol Cell Biol 24:4417-4427

Brennan J, Norris DP, Robertson EJ. 2002. **Nodal activity in the node governs left-right asymmetry**. Genes Dev 16: 2339-2344

Briscoe J, Ericson J. 1999. **The specification of neuronal identity by graded Sonic Hedgehog signalling**. Semin Cell Dev Biol 10: 353-362

Brokaw CJ. 2005. **Computer simulation of flagellar movement IX. Oscillation and symmetry breaking in a model for short flagella and nodal cilia**. Cell Motil Cytoskeleton 60: 35-47.

Brown NA, Wolpert L. 1990. **The development of handedness in left/right asymmetry**. Development 109: 1-9.

Campione M, Steinbeisser H, Schweickert A, Deissler K, van Bebber F, Lowe LA, Nowotschin S, Viebahn C, Haffter P, Kuehn MR, Blum M. 1999. **The homeobox gene Pitx2: mediator of asymmetric left-right signaling in vertebrate heart and gut looping**. Development 126: 1225-1234.

Cartwright JH, Piro O, Tuval I. 2004. **Fluid-dynamical basis of the embryonic development of left-right asymmetry in vertebrates**. Proc Natl Acad Sci USA 101: 7234-7239.

Caspary T, Larkins CE, Anderson KV. 2007. **The graded response to Sonic Hedgehog depends on cilia architecture**. Dev Cell12(5): 767-78

Chapman SC, Collignon J, Schoenwolf GC, Lumsden A. 2001. **Improved method for chick whole-embryo culture using a filter paper carrier**. Dev Dyn. 220(3): 284-9

Chen W, Burgess S, Hopkins N. 2001. **Analysis of the zebrafish smoothened mutant reveals conserved and divergent functions of hedgehog activity**. Development 128: 2385–2396.

Chen JK, Taipale J, Cooper MK, Beachy PA. 2002. **Inhibition of Hedgehog signaling by direct binding of cyclopamine to Smoothened**. Genes Dev 16: 2743–2748.

Cheng AMS, Thisse B, Thisse C, Wright CVE. 2000. **The lefty-related factor Xatv acts as a feedback inhibitor of Nodal signaling in mesoderm induction and L-R axis development in Xenopus**. Development 127: 1049-1061

Cheng SK, Olale F, Bennett JT, Brivanlou AH, Schier AF. 2003. **EGF-CFC proteins are essential coreceptors for the TGF-signals Vg1 and GDF1**. Genes Dev 17: 31-36

Chiang C, Litingtung Y, Lee E, Young KE, Corden JL, Westphal H, Beachy PA. 1996. **Cyclopia and defective axial patterning in mice lacking Sonic hedgehog gene function**. Nature 383: 407-413

Chuang P, McMahon A. 1999. **Vertebrate Hedgehog signalling modulated by induction of a Hedgehog-binding protein**. Nature 397: 617-621.

Chuang PT, Kawcak T, McMahon AP. 2003. **Feedback control of mammalian Hedgehog signaling by the Hedgehogbinding protein, Hip1, modulates Fgf signaling during branching morphogenesis of the lung**. Genes Dev 17: 342-347

Ciruna B, Rossant J. 2001. **FGF signaling regulates mesoderm cell fate specification and morphogenetic movement at the primitive streak**. Dev Cell 1: 37-49

Collignon J, Varlet I, Robertson EJ. 1996. **Relationship between asymmetric nodal expression and the direction of embryonic turning**. Nature 381: 155-158

Cooke J. 1995. **Vertebrate embryo handedness**. Nature 374(6524): 681

Corbit KC, Aanstad P, Singla V, Norman AR, Stainier DY, Reiter JF. 2005. **Vertebrate Smoothened functions at the primary cilium**. Nature 437(7061): 1018-21

Cornesse Y, Pieler T, Hollemann T. 2005. **Olfactory and lens placode formation is controlled by the hedgehog-interacting protein (Xhip) in Xenopus**. Dev Biol 277(2): 296-315

Dathe V, Gamel A, Manner J, Brand-Saberi B, Christ B. 2002. **Morphological left-right asymmetry of Hensen's node precedes the asymmetric expression of Shh and Fgf8 in the chick embryo**. Anat Embryol (Berl) 205: 343-354

Deng CX, Wynshaw-Boris A, Shen MM, Daugherty C, Ornitz DM, Leder P. 1994. **Murine FGFR-1 is required for early postimplantation growth and axial organization**. Genes Dev. 8: 3045-57

Eberhardt M. 2008. **L-R Achsenentwicklung in *Xenopus laevis*: Manipulation des asymmetrischen, Cilien-basierten Flüssigkeitsstroms und dessen Auswirkung auf die Genexpression der Wachstumsfakoren *XNr1* und *Coco* in der embryonalen Mittellinie**. Universität Hohenheim

Echelard Y, Epstein DJ, St-Jacques B, Shen L, Mohler J, McMahon JA, McMahon AP. 1993. **Sonic hedgehog, a member of a family of putative signaling molecules, is implicated in the regulation of CNS polarity**. Cell 75: 1417-30

Essner JJ, Vogan KJ, Wagner MK, Tabin CJ, Yost HJ, Brueckner M. 2002. **Conserved function for embryonic nodal cilia**. Nature 418: 37-38.

Essner JJ, Amack JD, Nyholm MK, Harris EB, Yost HJ. 2005. **Kupffer's vesicle is a ciliated organ of asymmetry in the zebrafish embryo that initiates left-right development of the brain, heart and gut**. Development 132: 1247-1260

Fischer A, Viebahn C, Blum M. 2002. **FGF8 acts as a right determinant during establishment of the left-right axis in the rabbit**. Curr Biol 12: 1807-1816

Feistel K. 2006. **Determination of Laterality in the Rabbit Embryo: Studies on Ciliation and Asymmetric Signal Transfer**. Universität Hohenheim.

Feistel K, Blum M. 2006**. Three types of cilia including a novel 9+4 axoneme on the notochordal plate of the rabbit embryo**. Dev Dyn 235(12): 3348-58

Feistel K, Blum M. 2008. **Gap junctions relay FGF8-mediated right-sided repression of Nodal in rabbit**. Dev Dyn. Epub ahead of print

Gaio U, Schweickert A, Fischer A, Garratt AN, Muller T, Ozcelik C, Lankes W, Strehle M, Britsch S, Blum M, Birchmeier C. 1999. **A role of the cryptic gene in the correct establishment of the left-right axis**. Curr Biol 9: 1339-1342

Hamada H. 2008. **Breakthroughs and future challenges in left-right patterning**. Develop Growth Differ 50: S71-S78

Hamada H, Meno C, Watanabe D, Saijoh Y. 2002. **Establishment of vertebrate left-right asymmetry**. Nat Rev Genet 3: 103-113

Hamburger V, Hamilton HL. 1992. **A series of normal stages in the development of the chick embryo**. Dev Dyn 195: 231-272

Hashimoto H, Rebagliati M, Ahmad N, Muraoka O, Kurokawa T, Hibi M, Suzuki T. 2004. **The Cerberus/Dan-family protein Charon is a negative regulator of Nodal signaling during left–right patterning in zebrafish**. Development 131: 1741-1753

Haycraft CJ, Banizs B, Aydin-Son Y, Zhang Q, Michaud EJ, Yoder BK. 2005. **Gli2 and Gli3 localize to cilia and require the intraflagellar transport protein polaris for processing and function**. PLoS Genet 1(4): e53

Heemskerk J, DiNardo S. 1994. **Drosophila hedgehog acts as a morphogen in cellular patterning**. Cell 76: 449-460

Herrmann BG, Kispert A. 1994. **The T genes in embryogenesis**. Trends Genet 10: 280-286

Hirokawa N, Tanaka Y, Okada Y, Takeda S. 2006. **Nodal flow and the generation of left-right asymmetry**. Cell 125: 33-45

Houde C, Dickinson R, Houtzager VM, Cullum R, Montpetit R, Metzler M, Simpson EM, Roy S, Hayden MR, Hoodless PA, Nicholson DW. 2006. **Hippi is essential for node cilia assembly and Sonic hedgehog signaling**. Dev Biol 300 (2): 523-33

Huangfu D, Liu A, Rakeman AS, Murcia NS, Niswander L, Anderson KV. 2003. **Hedgehog signalling in the mouse requires intraflagellar transport proteins**. Nature 426(6962): 83-7

Huangfu D, Anderson KV. 2005. **Cilia and Hedgehog responsiveness in the mouse**. Proc Natl Acad Sci USA 102(32): 11325-30

Huangfu D, Anderson KV. 2006. **Signaling from Smo to Ci/Gli: conservation and divergence of Hedgehog pathways from Drosophila to vertebrates**. Development 133(1): 3–14

Ingham PW, McMahon AP. 2001. **Hedgehog signaling in animal development: paradigms and principles**. Genes Dev 15: 3059-3087

Jeong J, McMahon AP. 2005. **Growth and pattern of the mammalian neural tube are governed by partially overlapping feedback activities of the hedgehog antagonists patched 1 and Hhip1**. Development 132: 143–154

Jia J, Jiang J. 2006. **Decoding the Hedgehog signal in animal development**. Cell Mol Life Sci 63(11): 1249-65

Jones CM, Kuehn MR, Hogan BL, Smith JC, Wright CV. 1995**. Nodal-related signals induce axial mesoderm and dorsalize mesoderm during gastrulation**. Development 121: 3651-3662

Karp SJ, Schipani E, St-Jacques B, Hunzelman J, Kronenberg H, McMahon AP. 2000. **Indian hedgehog coordinates endochondral bone growth and morphogenesis via parathyroid hormone related-protein-dependent and -independent pathways**. Development 127: 543–548

Keeler RF, Binns W. 1968. **Teratogenic compounds of Veratrum californicum (Durand). V. Comparison of cyclopian effects of steroidal alka- loids from the plant and structurally related compounds from other sources**. Teratology 1: 5-10.

Kiprilov EN, Awan A, Desprat R, Velho M, Clement CA, Byskov AG, Andersen CY, Satir P, Bouhassira EE, Christensen ST, Hirsch RE. 2008. **Human embryonic stem cells in culture possess primary cilia with hedgehog signaling machinery**. J Cell Biol 180(5): 897-904

Kramer-Zucker AG, Olale F, Haycraft CJ, Yoder BK, Schier AF, Drummond IA. 2005. **Cilia-driven fluid flow in the zebrafish pronephros, brain and Kupffer's vesicle is required for normal organogenesis**. Development 132: 1907-1921

Krauss, S., Concordet, J.-P., and Ingham, P.W. 1993. **A functionally conserved homolog of the Drosophila segment polarity gene hedgehog is expressed in tissues with polarising activity in zebrafish embryos**. Cell 75: 1431-1444

Lee SJ. 1990. **Identification of a novel member of the transforming growth factor-β superfamily**. Mol Endocrinol 4: 1034-1040.

Lee JD, Anderson KV. 2008. **Morphogenesis of the node and notochord: The cellular basis for the establishment and maintenance of left-right asymmetry in the mouse**. Dev Dyn. Epub ahead of print

Levin M, Johnson R, Stern C, Kuehn M, Tabin C. 1995. **A molecular pathway determining left–right asymmetry in chick embryogenesis**. Cell 82: 803-814

Liu A, Wang B, Niswander LA. 2005. **Mouse intraflagellar transport proteins regulate both the activator and repressor functions of Gli transcription factors**. Development 132(13): 3103-11

Logan M, Pagán-Westphal SM, Smith DM, Paganessi L, Tabin CJ. 1998. **The transcription factor Pitx2 mediates situs-specific morphogenesis in response to left-right asymmetric signals**. Cell 94: 307-317

Long S, Ahmad N, Rebagliati M. 2003. **The zebrafish nodal-related gene southpaw is required for visceral and diencephalic left-right asymmetry**. Development 130: 2303-2316

Lowe LA, Supp DM, Sampath K, Yokoyama T, Wright CV, Potter SS, Overbeek P, Kuehn MR. 1996. **Conserved left-right asymmetry of nodal expression and alterations in murine situs inversus**. Nature 381: 158-161

Mann RK, Beachy PA. 2004. **Novel lipid modifications of secreted protein signals**. Annu Rev Biochem 73: 891-923

Männer J. 2001. **Does an equivalent of the "ventral node" exist in chick embryos? A scanning electron microscopic study**. Anat Embryol (Berl) 203(6): 481-90

Marques S, Borges AC, Silva AC, Freitas S, Cordenonsi M, Belo JA. 2004. **The activity of the Nodal antagonist Cerl-2 in the mouse node is required for correct L/R body axis**. Genes Dev. 18: 2342-2347

Massague J. 2003. **Integration of Smad and MAPK pathways: a link and a linker revisited**. Genes Dev 17: 2993-2997

Meno C, Shimono A, Saijoh Y, Yashiro K, Mochida K, Ohishi S, Noji S, Kondoh H, Hamada H. 1998. **lefty-1 is required for left-right determination as a regulator of lefty-2 and nodal**. Cell 94: 287-297

Meno C, Gritsman K, Ohishi S, Ohfuji Y, Heckscher E, Mochida K, Shimono A, Kondoh H, Talbot WS, Robertson EJ, Schier AF, Hamada H. 1999. **Mouse Lefty2 and zebrafish antivin are feedback inhibitors of nodal signaling during vertebrate gastrulation**. Mol Cell 4: 287-298

Meyers EN, Martin GR. 1999. **Differences in left-right axis pathways in mouse and chick: functions of FGF8 and SHH**. Science 285: 403-406

Mitchell B, Jacobs R, Li J, Chien S, Kintner C. 2007. **A positive feedback mechanism governs the polarity and motion of motile cilia**. Nature 447(7140): 97-101

Mohammadi M, McMahon G, Sun L, Tang C, Hirth P, Yeh BK, Hubbard SR, Schlessinger J. 1997. **Structures of the tyrosine kinase domain of fibroblast growth factor receptor in complex with inhibitors**. Science 276: 955-960

Monsoro-Burq A, Le Douarin NM. 2001. **BMP4 plays a key role in left-right patterning in chick embryos by maintaining Sonic Hedgehog asymmetry**. Mol Cell 4: 789-99

Neugebauer J, Amack JD, Yost JH. 2008. **FGF signalling during embryo development regulates ciliogenesis in diverse epithelia**. Dev Biol 319: 522. Abstract.

Nonaka S, Tanaka Y, Okada Y, Takeda S, Harada A, Kanai Y, Kido M, Hirokawa N. 1998. **Randomization of left-right asymmetry due to loss of nodal cilia generating leftward flow of extraembryonic fluid in mice lacking KIF3B motor protein**. Cell 95: 829-837

Nonaka S, Shiratori H, Saijoh Y, Hamada H. 2002. **Determination of left-right patterning of the mouse embryo by artificial nodal flow**. Nature 418: 96-99

Nonaka S, Yoshiba S, Watanabe D, Ikeuchi S, Goto T, Marshall WF, Hamada H. 2005. **De novo formation of left-right asymmetry by posterior tilt of nodal cilia**. PLoS Biol 3: e268

Norris DP, Brennan J, Bikoff EK, Robertson EJ. 2002. **The Foxh1-dependent autoregulatory enhancer controls the level of Nodal signals in the mouse embryo**. Development 129: 3455-3468

Norris DP, Robertson EJ. 1999. **Asymmetric and node-specific nodal expression patterns are controlled by two distinct cis-acting regulatory elements**. Genes Dev 13: 1575-1588

Nüsslein-Volhard C, Wieschaus E. 1980. **Mutations affecting segment number and polarity in Drosophila**. Nature 287: 795-801

Ochi H, Pearson BJ, Chuang PT, Hammerschmidt M, Westerfield M. 2006. **Hhip regulates zebrafish muscle development by both sequestering Hedgehog and modulating localization of Smoothened**. Dev Biol 297(1): 127-40

Ohi Y, Wright CV. 2007. **Anteriorward shifting of asymmetric Xnr1 expression and contralateral communication in left-right specification in Xenopus**. Dev Biol. 301(2): 447-63

Okada Y, Nonaka S, Tanaka Y, Saijoh Y, Hamada H, Hirokawa N. 1999. **Abnormal nodal flow precedes situs inversus in iv and inv mice**. Mol Cell 4: 459-468

Okada Y, Takeda S, Tanaka Y, Belmonte JC, Hirokawa N. 2005. **Mechanism of nodal flow: a conserved symmetry breaking event in left-right axis determination**. Cell 121: 633-644

Onuma Y, Yeo CY, Whitman M. 2006. **XCR2, one of three Xenopus EGF-CFC genes, has a distinct role in the regulation of left-right patterning**. Development 133: 237-250

Pagán-Westphal SM, Tabin CJ. 1998. **The transfer of left-right positional information during chick embryogenesis**. Cell 93: 25-35

Park TJ, Haigo SL, Wallingford JB. 2006. **Ciliogenesis defects in embryos lacking inturned or fuzzy function are associated with failure of planar cell polarity and Hedgehog signaling**. Nat Genet 38(3): 303-11

Park TJ, Mitchell BJ, Abitua PB, Kintner C, Wallingford JB. 2008. **Dishevelled controls apical docking and planar polarization of basal bodies in ciliated epithelial cells**. Nat Genet 40(7): 871-9

Parmantier E, Lynn B, Lawson D, Turmaine M, Namini S, Chakrabarti L, McMahon A, Jessen K, Mirsky R. 1999. **Schwann cell-derived Desert hedgehog controls the development of peripheral nerve sheaths**. Neuron 23: 713-724

R Development Core Team. 2008. R: **A language and environment for statistical computing. R Foundation for Statistical Computing**, Vienna, Austria. ISBN 3-900051-07-0, http://www .R-project .org.

Rankin CT, Bunton T, Lawler AM, Lee SJ. 2000. **Regulation of left–right patterning in mice by growth/differentiation factor-1**. Nat Genet 24: 262-265

Rebagliati MR, Toyama R, Fricke C, Haffter P, Dawid IB. 1998. **Zebrafish nodal-related genes are implicated in axial patterning and establishing left-right asymmetry**. Dev Biol 199: 261-272

Riddle, R., Johnson, R., Laufer, E., and Tabin, C. 1993. **Sonic hedgehog mediates the polarizing activity of the ZPA**. Cell 75: 1401-1416

Roelink H, Augsburger A, Heemskerk J, Korzh V, Norlin S, Ruiz i Altaba A, Tanabe Y, Placzek M, Edlund T, Jessell TM, Dodd J. 1994. **Floor plate and motor neuron induction by vhh-1, a vertebrate homolog of hedgehog expressed by the notochord**. Cell. 76: 761-75

Rohatgi R, Milenkovic L, Scott MP. 2007. **Patched1 Regulates Hedgehog Signaling at the Primary Cilium**. Science 317: 372-76

Ryan AK, Blumberg B, Rodriguez-Esteban C, Yonei-Tamura S, Tamura K, Tsukui T, de la Pena J, Sabbagh W, Greenwald J, Choe S, Norris DP, Robertson EJ, Evans RM, Rosenfeld MG, Izpisúa Belmonte JC. 1998. **Pitx2 determines left-right asymmetry of internal organs in vertebrates**. Nature 394: 545-551

Saijoh Y, Oki S, Ohishi S, Hamada H. 2003. **Left-right patterning of the mouse lateral plate requires nodal produced in the node**. Dev Biol 256: 160-172

Saijoh Y, Oki S, Tanaka C, Nakamura T, Adachi H, Yan YT, Shen MM, Hamada H. 2005. **Two nodal-responsive enhancers control left-right asymmetric expression of Nodal**. Dev Dyn 232: 1031-1036

Sampath K, Cheng AMS, Frisch A, Wright CVE. 1997. **Functional differences among Xenopus nodal-related genes in left-right axis determination**. Development 124: 3293-3302

Satir P, Christensen ST. 2007. **Overview of Structure and Function of Mammalian Cilia**. Annu Rev Physiol 69: 377-400

Sbalzarini IF, Koumoutsakos P. 2005. **Feature point tracking and trajectory analysis for video imaging in cell biology**. J Struct Biol 151(2): 182-95

Schier AF, Shen MM. 2000. **Nodal signalling in vertebrate development**. Nature 403: 385-389

Schilling TF, Concordet JP, Ingham PW. 1999. **Regulation of left-right asymmetries in the zebrafish by Shh and BMP4**. Dev Biol 210: 277-287

Schneider I. 2008. **Die Rolle des FGF-Signalwegs in der Links-Rechts-Achsenentwicklung von *Xenopus laevis***. Universität Hohenheim

Scholey J. 2008. **Intraflagellar transport motors in cilia: moving along the cell's antenna**. JCB 180(1): 23-29

Schweickert A, Weber T, Beyer T, Vick P, Bogusch S, Feistel K, Blum M. 2007. **A cilia-driven leftward flow specifies laterality upstream of asymmetric Nodal signaling in the frog Xenopus laevis**. Curr Biol: 17(1): 60-6

Shook DR, Majer C, Keller R. 2004. **Pattern and morphogenesis of presumptive superficial mesoderm in two closely related species, Xenopus laevis and Xenopus tropicalis**. Dev Biol 270: 163-185

Simons M, Gloy J, Ganner A, Bullerkotte A, Bashkurov M, Krönig C, Schermer B, Benzing T, Cabello OA, Jenny A, Mlodzik M, Polok B, Driever W, Obara T, Walz G. 2005. **Inversin, the gene product mutated in nephronophthisis type II, functions as a molecular switch between Wnt signaling pathways**. Nat Genet. 37(5):537-43

Simons M, Mlodzik M. 2008. **Planar Cell Polarity Signaling: From Fly Development to Human Disease**. Annu Rev Genet. Epub ahead of print

St-Jacques B, Hammerschmidt M, McMahon A. 1999. **Indian hedgehog signaling regulates proliferation and differentiation of chondrocytes and is essential for bone formation**. Genes & Dev. 13: 2072-2086

Sulik K, Dehart DB, Iangaki T, Carson JL, Vrablic T, Gesteland K, Schoenwolf GC. 1994. **Morphogenesis of the murine node and notochordal plate**. Dev Dyn 201: 260-278

Sun X, Meyers EN, Lewandoski M, Martin GR. 1999. **Targeted disruption of Fgf8 causes failure of cell migration in the gastrulating mouse embryo**. Genes Dev 13: 1834-46

Supp DM, Witte DP, Potter SS, Brueckner M. 1997. **Mutation of an axonemal dynein affects left-right asymmetry in inversus viscerum mice**. Nature 389: 963-966

Tanaka Y, Okada Y, Hirokawa N. 2005. **FGF-induced vesicular release of Sonic hedgehog and retinoic acid in leftward nodal flow is critical for left-right determination**. Nature 435: 172-177

Thisse B, Thisse C. 2005. **Functions and regulations of fibroblast growth factor signaling during embryonic development**. Dev Biol 287: 390-402

Tsang TE, Kinder SJ, Tam PP. 1999. **Experimental analysis of the emergence of left-right asymmetry of the body axis in early postimplantation mouse embryos**. Cell Mol Biol 45: 493-503

Tsukui T, Capdevila J, Tamura K, Ruiz-Lozano P, Rodriguez- Esteban C, Yonei-Tamura S, Magallon J, Chandraratna RA, Chien K, Blumberg B. 1999. **Multiple left-right asymmetry defects in Shh(/) mutant mice unveil a convergence of the shh and retinoic acid pathways in the control of Lefty-1**. Proc Natl Acad Sci USA 96: 11376-11381

van den Heuvel M, Ingham PW. 1996. **smoothened encodes a serpentine protein required for hedgehog signaling**. Nature 382: 547–551

Varga ZM, Amores A, Lewis KE, Yan YL, Postlethwait JH, Eisen JS, Westerfield M. 2001. **Zebrafish smoothened functions in ventral neural tube specification and axon tract formation**. Development 128(18): 3497-509

Viebahn C, Mayer B, Hrabe de Angelis M. 1995. **Signs of the principle body axes prior to primitive streak formation in the rabbit embryo**. Anat Embryol (Berl) 192(2): 159-69

Vierkotten J, Dildrop R, Peters T, Wang B, Ruther U. 2007. **Ftm is a novel basal body protein of cilia involved in Shh signalling**. Development 134: 2569-2577

Vonica A, Brivanlou AH. 2007. **The left-right axis is regulated by the interplay of Coco, Xnr1 and derrière in *Xenopus* embryos**. Dev Biol 303: 281-294

Vortkamp A, Lee K, Lanske B, Segre GV, Kronenberg HM, Tabin C. 1996. **Indian hedgehog and parathyroid hormone-related protein regulate the rate of cartilage differentiation**. Science 273: 613-622

Weber T. 2006. **Charakterisierung einer durch Cilien angetriebenen vektoriellen Flüssigkeitsströmung in *Xenopus laevis* zur Brechung der bilateralen Symmetrie**. Universität Hohenheim

Wemmer KA, Marshall WF. 2004. **Flagellar motility: all pull together**. Curr Biol 14: R992-993

Whitman M, Mercola M. 2001. **TGF-beta superfamily signaling and left-right asymmetry**. Sci STKE 2001: RE1

Yamaguchi TP, Harpal K, Henkemeyer M, Rossant J. 1994. **fgfr-1 is required for embryonic growth and mesodermal patterning during mouse gastrulation**. Genes Dev 8: 3032-44

Yamamoto M, Mine N, Mochida K, Sakai Y, Saijoh Y, Meno C, Hamada H. 2003. **Nodal signaling induces the midline barrier by activating Nodal expression in the lateral plate**. Development 130: 1795-1804

Ybot-Gonzalez P, Savery D, Gerrelli D, Signore M, Mitchell CE, Faux CH, Greene ND, Copp AJ. 2007. **Convergent extension, planar-cell-polarity signalling and initiation of mouse neural tube closure**. Development 134(4): 789-99

Yokoi H, Shimada A, Carl M, Takashima S, Kobayashi D, Narita T, Jindo T, Kimura T, Kitagawa T, Kage T, Sawada A, Naruse K, Asakawa S, Shimizu N, Mitani H, Shima A, Tsutsumi M, Hori H, Wittbrodt J, Saga Y, Ishikawa Y, Araki K, Takeda H. 2006. **Mutant analyses reveal different functions of fgfr1 in medaka and zebrafish despite conserved ligand-receptor relationships**. Dev Biol 304(1): 326-37

Zhang X M, Ramelho-Santos M, McMahon AP. 2001. **Smoothened mutants reveal redundant roles for Shh and Ihh signaling including regulation of L/R asymmetry by the mouse node**. Cell 105: 781-792

Zhou X, Sasaki H, Lowe L, Hogan BL, Kuehn MR. 1993. **Nodal is a novel TGF-beta-like gene expressed in the mouse node during gastrulation**. Nature 361: 543-547

Bei Prof. Dr. Martin Blum möchte ich mich ganz herzlich für die Chance, diese Doktorarbeit in seiner Arbeitsgruppe durchführen zu können, sowie für sein fortwährendes Engagement und seine Motivation bedanken.

Prof. Dr. Heinz Breer danke ich für sein Interesse an dieser Arbeit, sowie die von ihm investierte Zeit.

Ich bedanke mich ganz herzlich bei Dr. Anja Rietema, von der ich nicht nur labor-technisch sondern auch „tierisch“ viel gelernt habe.

Bei allen ZVHlern, besonders bei Dr. Jutta Mönchenberg möchte ich mich für die nette Zeit und die sehr gute Zusammenarbeit bedanken.

Vielen Dank an alle Kollegen! Es war eine klasse Zeit mit euch und ich werde nicht nur meinen Schreibtisch an der Kaffeemaschine/Kuchenablageplatz sehr vermissen! Besonders bedanken möchte ich mich bei Thomas Weber, durch den die professionellen Flow-Analysen überhaupt erst möglich waren (ich war gerne dein DAU!) und bei Dr. Kerstin Feistel für die „blinde“ Zusammenarbeit und das viele Lesen und Korrigieren dieser Arbeit.

Vielen lieben Dank meiner Familie für all die Unterstützung, Geduld und den großen Rückhalt. Ein großes Dankeschön gilt dabei vor allem auch Tommy für seine unglaubliche Unterstützung und dafür, dass er immer an mich glaubt.